

ABSTRACT

SITU, XINGCI. Investigations of Photosensitizer Structure-Activity Relationships for Photodynamic Inactivation of Pathogenic Yeast. (Under the direction of Dr. Reza A. Ghiladi).

Opportunistic pathogenic yeast strains can cause life-threatening infections in immunocompromised individuals. Herein, we studied the *in vitro* antimicrobial photodynamic inactivation (aPDI) of nine photosensitizers (PS) of different chemical and physical properties, including charge and size, against pathogenic *Candida* and *Cryptococcus* fungi to survey the structure-activity relationships of photosensitizers for potential use in antifungal applications. Photodynamic therapy employs a photosensitizer, visible light, and molecular oxygen to produce cytotoxic reactive oxygen species (ROS) that lead to apoptosis. Our results demonstrated that yeast belonging to the genus *Candida* were susceptible to both cationic and anionic photosensitizers, whereas those belonging to the genus *Cryptococcus* only showed photoinactivation towards cationic ones. The difference in photosensitizer efficacy was rationalized in light of electrostatic interactions between the yeast cell membrane and the photosensitizer: the negatively charged membrane of *Cryptococcus* led to unfavorable interactions with anionic PS, whereas the neutral cell membrane of *Candida* led to more favorable interactions with both cationic and anionic PS. We also explored the *in vitro* photodynamic efficacy of cellulose nanocrystal-porphyrin conjugates as potential disinfective materials to prevent the surface transmission of pathogenic microbials. Overall, the results for both solution-based and materials-based photosensitizers demonstrated that aPDT can exhibit broad spectrum antifungal activity.

© Copyright 2013 Xingci Situ

All Rights Reserved

Investigation of Photosensitizer Structure-Activity Relationships for Photodynamic
Inactivation of Pathogenic Yeast

by
Xingci Situ

A thesis submitted to the Graduate Faculty of
North Carolina State University
in partial fulfillment of the
requirements for the Degree of
Master of Science

Chemistry

Raleigh, North Carolina

2013

APPROVED BY:

Walter W. Weare

Elon A. Ison

Reza A. Ghiladi
Chair of Advisory Committee

DEDICATION

I dedicate this work to my family and friends for all the love and support.

BIOGRAPHY

Xingci Situ was born on September 1988. She grew up in Guangdong, China, and then immigrated with her family to the United States at the age of 12. She and her family settled down in Sacramento, California. She graduated from C. K. McClatchy High School, Sacramento, CA in 2006, and was accepted into University of California, Santa Cruz, where she majored in Chemistry. She worked as an undergraduate researcher in Dr. Scott Oliver's group on the synthesis of organometallic mesoporous materials. In summer 2010, she did summer research internship in Münster, Germany. After graduated from UCSC in 2011 with a Bachelor of Science in Chemistry, she continues graduate education in the Department of Chemistry in North Carolina State University under the direction of Dr. Reza A. Ghiladi.

ACKNOWLEDGMENTS

I would like to express my deepest gratitude to Dr. Reza A. Ghiladi for all his mentorships and supports for the past 2.5 years. Reza provides a positive lab environment that is supportive and encouraging to the students. He offers the freedom and independence to explore science but also provides guidance whenever is needed. I am grateful for being part of the Ghiladi group. I would also like to thank all past and current members of the Ghiladi group, Nikolette Lucas, Leah Carey, and Roman Gavenko, for making my days in the lab more fun and interesting. Special thanks to Dr. David A. Barrios and Brad Carpenter for all their help and support throughout the years. I thank all my family and friends for their unconditional love and always by my side. Without all of you, I would not be able to accomplish this journey and become who I am today.

TABLE OF CONTENTS

LIST OF TABLES	vi
LIST OF FIGURES	vii
CHAPTER 1. GENERAL INTRODUCTION	
1.1 Impacts of fungal infections.....	1
1.2 Photodynamic therapy.....	2
1.3 Mechanism of photodynamic therapy.....	3
1.4 Antimicrobial photodynamic therapy.....	4
1.5 Motivation.....	6
References.....	7
 CHAPTER 2. SURVEY OF PHOTSENSITIZER STRUCTURE-ACTIVITY RELATIONSHIPS FOR <i>IN VITRO</i> PHOTODYNAMIC THERAPY OF PATHOGENIC YEAST	
2.1 Abstract.....	11
2.2 Introduction.....	12
2.3 Materials and Methods.....	14
2.4 Results and Discussion.....	18
2.4.1 Photoactivity of cationic photosensitizers.....	19
2.4.2 Photoactivity of anionic photosensitizers.....	25
2.5 Conclusions.....	31
References.....	32
 CHAPTER 3. CELLULOSE NANOCRYSTAL-PORPHYRIN CONJUGATES AND THEIR ANTIFUNGAL PROPERTIES	
3.1 Abstract.....	35
3.2 Introduction.....	36
3.3 Materials and Methods.....	39
3.4 Results and Discussion.....	41
3.4.1 aPDT Studies with CatPor and CNC-CatPor.....	42
3.4.2 aPDT Studies with AnPor and CNC-AnPor.....	47
3.5 Conclusions.....	52
References.....	53

LIST OF TABLES

Table 2.1	Selected properties of the photosensitizers that affect PDT activity.....	16
-----------	---	----

LIST OF FIGURES

Figure 1.1	Mechanism of photodynamic therapy.....	4
Figure 2.1	Chemical structures of common antifungal drugs for systemic mycoses infection: (a) amphotericin B, (b) 5-fluorocytosin, (c) miconazole, (d) ketoconazole, (e) fluconazole, (f) itraconazole.....	13
Figure 2.2	Chemical structures of photosensitizers employed in this study.....	16
Figure 2.3	Structures of cryptococcal capsular polysaccharides, glucuronoxylomannan (GXM) and galactoxylomannan (GalXM).....	22
Figure 2.4	Photoinactivation of <i>Candida albicans</i> with cationic photosensitizers (A) MB, (B) JB461, (C) TMPyP, (D) TMNAP.....	23
Figure 2.5	Photoinactivation of <i>Candida glabrata</i> with cationic photosensitizers (A) MB, (B) JB461, (C) TMPyP, (D) TMNAP.....	24
Figure 2.6	Photoinactivation of <i>Cryptococcus neoformans</i> with cationic photosensitizers (A) MB, (B) JB461, (C) TMPyP, (D) TMNAP.....	25
Figure 2.7	Photoinactivation of <i>Candida albicans</i> with anionic photosensitizers (E) TSPP, (F) TCPP-PD, (G) RB, (H) B23, (I) PhCS.....	28
Figure 2.8	Photoinactivation of <i>Candida glabrata</i> with anionic photosensitizers (E) TSPP, (F) TCPP-PD, (G) RB, (H) B23, (I) PhCS.....	29
Figure 2.9	Photoinactivation of <i>Cryptococcus neoformans</i> . <i>C. neoformans</i> were with anionic photosensitizers (E) TSPP, (F) TCPP-Pd, (G) RB, (H) B23, (I) PhCS.....	30
Figure 3.1	Synthesis of cellulose nanocrystal-porphyrin (CNC-por) conjugates.....	39
Figure 3.2	Photodynamic inactivation of <i>Candida albicans</i> with (A) water-soluble CatPor and (B) CNC-CatPor.....	43
Figure 3.3	Photodynamic inactivation of <i>C. neoformans</i> with (A) water-soluble CatPor and (B) CNC-CatPor.....	45

Figure 3.4	Photodynamic inactivation of <i>C. neoformans</i> with 200 μ M of CNC-CatPor..	47
Figure 3.5	Photodynamic inactivation of <i>C. albicans</i> with (A) water soluble AnPor and (B) CNC-AnPor.	48
Figure 3.6	Photodynamic inactivation of <i>C. albicans</i> with 30 μ M CNC-AnPor.....	49
Figure 3.7	Photodynamic inactivation of <i>C. neoformans</i> with (A) water soluble AnPor and (B) CNC-AnPor.....	51

CHAPTER 1

General Introduction

1.1 Impacts of fungal infections

Over the past several decades, the incidence rates of fungal infections have increased dramatically.¹ According to Martin *et al.*, an epidemiological study in the United States reported that the cases of lethal infection caused by fungal pathogens increased by 207% between 1979 and 2000.² Opportunistic fungal pathogens, such as those belonging to the genera *Candida*, *Cryptococcus*, and *Aspergillus*, can cause superficial or invasive infections which are life threatening, especially to patients with compromised immune systems.³⁻⁶ *Candida* pathogens are responsible for ~80% of systemic fungal infections, are the fourth leading cause of blood stream infection in hospitals, and have a crude mortality rate of ~50%.^{1,7-13} Cryptococcosis is caused by the encapsulated *Cryptococcus neoformans*, and can be acquired through inhalation of the airborne pathogen from the environment. Nearly 1 million HIV/AIDS patients are diagnosed with cryptococcal meningitis annually, resulting in 625,000 deaths.^{14,15} Treatments for such infections require taking multiple antifungal drugs for prolonged periods of time, with recurrence of infections being often observed, and which contributes to the development of resistance to these antifungal medications.¹⁶ Despite the fact that fungal infections have such a significant impact on human health, the number and efficacy of antifungal drugs available are limited. Commercially available antifungal medications can cause serious side effects, lead to harmful drug-drug interactions, and in some cases are ineffective towards other yeast strains.¹⁷⁻¹⁹ As such, new treatments for

combatting the rise of pathogenic fungal infections, and in particular drug-resistant ones, are needed. Antimicrobial photodynamic inactivation of pathogenic fungal infections may prove to be such an alternative treatment.^{20,21}

1.2 Photodynamic therapy

Photodynamic therapy, PDT, was discovered by Oskar Raab from the Hermann von Tappeiner laboratory in the 1900s.²² He observed cell inactivation of *Paramecium caudatum*, a eukaryotic unicellular organism, after treatment with light and acridine. In the 1970s, PDT was developed as a therapeutic tool for cancer utilizing porphyrin-based photosensitizers.²³⁻²⁶ Since then, photodynamic therapy has evolved into an FDA-approved, minimally invasive medical treatment for disease conditions such as skin tumors,^{27,28} cutaneous T-cell lymphoma,²⁹ Barrett's esophagus, obstructing esophageal carcinoma, and early stages of cervical cancer.³⁰ Due to the increase of antibiotic/antifungal-resistant microbes, research efforts had been in developing new antimicrobial strategies. Only recently has PDT been intensively studied as an alternative treatment for infections, including acne vulgaris, leishmaniasis, wound infections, and oral infections. These studies have suggested that PDT may be applied more generally against localized infections caused by bacteria, fungi, and viruses, including drug-resistant strains, given its unique mode of action.^{20,25,31-34}

1.3 Mechanism of photodynamic therapy

Photodynamic therapy employs a non-toxic photosensitizer (PS) that upon exposure to visible light of appropriate wavelength corresponding to the absorption spectrum of the photosensitizer, ultimately leads to the formation of radicals or reactive oxygen species (ROS). These radicals/ROS have been shown to be biocidal, and at high enough concentration can lead to cell death. The specific details of the mechanism of action for photodynamic therapy are illustrated in Fig. 1.1. A ground state photosensitizer is promoted to the excited state upon absorption of light. This excited singlet state, with a half life of 10^{-6} to 10^{-9} s,^{35,36} either relaxes back to the ground state through fluorescence, or converts to triplet state through intersystem crossing. Cell inactivation can then be achieved by one of two pathways, the so called Type I or Type II mechanisms. The Type I mechanism involves transfer of an electron or hydrogen to produce reactive radical or superoxide species such as the hydroxyl radical or hydrogen peroxide. The type II mechanism proceeds via energy transfer from the excited (triplet) state PS to molecular oxygen (triplet in ground state), thereby generating singlet oxygen, an extremely reactive oxidant that can cause irreversible cellular damage.^{36,37} Singlet oxygen has a short lifetime (10^{-6}) so diffusivity is limited, and does not damage other tissues when effective PS localization occurs. The disadvantages of PDT include i) the photosensitizer can target healthy cells or tissue, ii) cell death is limited to the area where light applies (tissue penetration issues), iii) the photosensitizer may return to the ground state through phosphorescence and iv) the PS may be destroyed by photobleaching due to oxidation by the singlet oxygen produced.

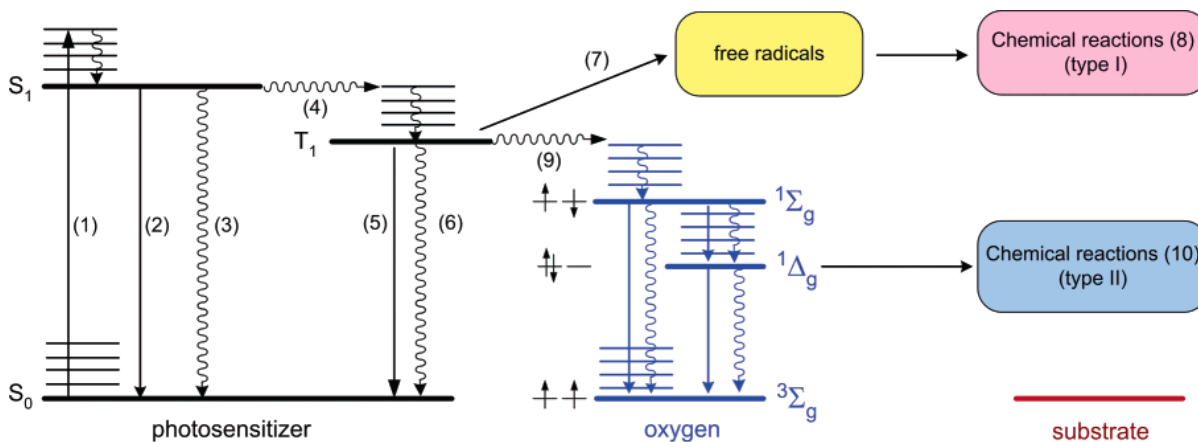


Figure 1.1. Mechanism of photodynamic therapy. Adapted from Szacilowski *et al.*³⁸

1.4 Antimicrobial photodynamic therapy (aPDT)

The increase of drug-resistant microbials has raised the interest of searching for new alternative treatments for pathogenic infections. The susceptibility of microorganisms to a photodynamic approach suggests that PDT appears to be a good candidate as an antimicrobial treatment. An advantage of aPDT is that there is no cellular defense against singlet oxygen, and therefore resistance to the application is unlikely to occur.³⁹ Antibacterial PDT has been studied extensively on both drug-susceptible and drug-resistant bacteria using a diverse class of photosensitizers, such as phenothiazinium dyes,⁴⁰ BODIPY-based compounds,⁴¹⁻⁴⁴ and tetrapyrroles.^{23,32,45-47} In general, anionic, cationic, and neutral sensitizers are effective for Gram-positive bacterial inactivation, whereas Gram-negative bacteria appear to be only susceptible towards cationic photosensitizers. The difference in susceptibility between these two classes of bacteria has been explained by the physiological and cellular structure variations between the Gram-positive and Gram-negative bacteria:

Gram-positive species contain permeable cell walls whereas Gram-negative species have an outer membrane that acts as an additional permeation barrier.^{48,49}

In contrast to antibacterial PDT, research on antifungal PDT has been more limited, and the PS used in these studies have not been as structurally diverse. The majority of antifungal PDT research efforts have focused on the genus *Candida* since it is the most prevalent yeast family with respect to human infections. Susceptibility of the *Candida* genus against a phenothiazine PS has been studied previously: a fungicidal effect was observed using the photosensitizer methylene blue (MB) at a concentration of 0.1 mg/mL upon illumination (fluence of 28 J/cm²) against various *Candida* species.⁵⁰ An *in vivo* study of photodynamic inactivation with 400 µg/mL of MB resulted in the total eradication of *C. albicans* on immunodeficient beige nude mice with oral azole-resistant candidiasis.⁵¹ Costa *et al.* studied the inactivation of *C. albicans* using rose bengal (RB) and erythrosine and observed 3.45 and 1.97 log units CFU reduction of planktonic cells, respectively, but <1 log unit CFU reduction for *C. albicans* within a biofilm.⁵² According to Dovigo *et al.*, biofilm-associated cells are less susceptible to aPDT than planktonic cells.⁵³ Cormick and coworkers investigated the *in vitro* photodynamic inactivation of *C. albicans* with 5 µM of 5,10,15,20-tetrakis(1-methyl-4-pyrid-4-yl)porphyrin with 30 min of visible light illumination, and achieved 5 log units CFU reduction.⁵⁴ Freeze-fracture electron microscopy of *C. albicans* cells treated with 5-phenyl-10,15,20-Tris(*N*-methyl-4-pyridyl)porphyrin chloride demonstrated, upon illumination, that photodamage was initiated from the outer leaflet of the plasma membrane to the inner leaflet.⁵⁵

1.5 Motivation

Overall, the above initial studies have shown that PDT holds great promise as an antifungal treatment; however, given the lack of systematic studies for antifungal PDT, many questions regarding the mode of action, PS structure-activity relationships, and breadth or scope of inactivation persist. Given the lack in understanding of antifungal PDT, and in light of the increases in incidence rates of drug-resistant pathogenic yeast infections and hospital acquired fungal infections that have resulted in corresponding high modality and mortality rates, there is a significant need for further research into aPDT as an alternative treatment for such infections. The aim of this research is to investigate the photodynamic inactivation mechanism of pathogenic fungi of different cellular compositions against photosensitizers of different photophysical and chemical properties, in order to expand our current knowledge of antifungal PDT through a systematic study that is the necessary foundation for the future development of potent antifungal photosensitizers.

REFERENCES

- (1) Beck-Sague, C.; Jarvis, W. R. *J Infect Dis* **1993**, *167*, 1247.
- (2) Martin, G. S.; Mannino, D. M.; Eaton, S.; Moss, M. *N Engl J Med* **2003**, *348*, 1546.
- (3) Garibotto, F. M.; Garro, A. D.; Masman, M. F.; Rodriguez, A. M.; Luiten, P. G.; Raimondi, M.; Zacchino, S. A.; Somlai, C.; Penke, B.; Enriz, R. D. *Bioorg Med Chem* **2010**, *18*, 158.
- (4) Currie, B. P.; Casadevall, A. *Clin Infect Dis* **1994**, *19*, 1029.
- (5) Espinel-Ingroff, A. *Rev Iberoam Micol* **2009**, *26*, 15.
- (6) Dolmans, D. E.; Fukumura, D.; Jain, R. K. *Nat Rev Cancer* **2003**, *3*, 380.
- (7) Wisplinghoff, H.; Bischoff, T.; Tallent, S.; Seifert, H.; Wenzel, R.; Edmond, M. *Clin Infect Dis* **2004**, *39*, 309
- (8) Edmond, M. B.; Wallace, S. E.; McClish, D. K.; Pfaller, M. A.; Jones, R. N.; Wenzel, R. P. *Clin Infect Dis* **1999**, *29*, 239.
- (9) Wey, S.; Mori, M.; Pfaller, M.; Woolson, R.; Wenzel, R. *Arch Intern Med* **1988**, *148*, 2642
- (10) Wenzel, R. P. *Clin Infect Dis* **1995**, *20*, 1531.
- (11) Nolla-Salas, J.; Sitges-Serra, A.; Leon-Gil, C.; Martinez-Gonzalez, J.; Leon-Regidor, M.; Ibanez-Lucia, P.; Torres-Rodriguez, J. *Intensive Care Med* **1997**, *23*, 23
- (12) Gonzalez de Molina, F.; Leon, C.; Ruiz-Santana, S.; Saavedra, P.; Group, t. C. I. S. *Critical Care* **2012**, *16*, R105.
- (13) Gudlaugsson, O.; Gillespie, S.; Lee, K.; Vande Berg, J.; Hu, J.; Messer, S.; Herwaldt, L.; Pfaller, M.; Diekema, D. *Clin Infect Dis* **2003**, *37*, 1172
- (14) Park, B. J.; Wannemuehler, K. A.; Marston, B. J.; Govender, N.; Pappas, P. G.; Chiller, T. M. *AIDS* **2009**, *23*, 525.
- (15) McNeil, M. M.; Nash, S. L.; Hajjeh, R. A.; Phelan, M. A.; Conn, L. A.; Plikaytis, B. D.; Warnock, D. W. *Clin Infect Dis* **2001**, *33*, 641.

- (16) d'Enfert, C. *Curr Opin Microbiol* **2009**, *12*, 358.
- (17) Espinel-Ingroff, A. In *Encyclopedia of Microbiology (Third Edition)*; Academic Press: Oxford, 2009, p 205.
- (18) Bell, A. S. In *Comprehensive Medicinal Chemistry II*; Elsevier: Oxford, 2007, p 445.
- (19) Kathiravan, M. K.; Salake, A. B.; Chothe, A. S.; Dudhe, P. B.; Watode, R. P.; Mukta, M. S.; Gadhwane, S. *Bioorg Med Chem* **2012**, *20*, 5678.
- (20) Hamblin, M. R.; Hasan, T. *Photochem Photobiol Sci* **2004**, *3*, 436.
- (21) Jori, G.; Fabris, C.; Soncin, M.; Ferro, S.; Coppellotti, O.; Dei, D.; Fantetti, L.; Chiti, G.; Roncucci, G. *Laser Surg Med* **2006**, *38*, 468.
- (22) Raab, O. *Z Biol-Munich* **1900**, *39*, 524.
- (23) Moan, J. *Photochem Photobiol* **1986**, *43*, 681.
- (24) Detty, M. R.; Gibson, S. L.; Wagner, S. J. *J Med Chem* **2004**, *47*, 3897.
- (25) Chabrier-Rosello, Y.; Foster, T. H.; Perez-Nazario, N.; Mitra, S.; Haidaris, C. G. *Antimicrob Agents Chemother* **2005**, *49*, 4288.
- (26) Dougherty, T. J. *J Clin Laser Med Surg* **1996**, *14*, 219.
- (27) Bagnato, V. S.; Kurachi, C.; Ferreira, J.; Marcassa, L. G.; Sibata, C. H.; Allison, R. R. *Photodiagn Photodyn* **2005**, *2*, 107.
- (28) Moreira, L. M.; dos Santos, F. V.; Lyon, J. P.; Maftoum-Costa, M.; Pacheco-Soares, C.; da Silva, N. S. *Aust J Chem* **2008**, *61*, 741.
- (29) Calzavara-Pinton, P. G.; Venturini, M.; Sala, R. *J Photochem Photobiol B* **2005**, *78*, 1.
- (30) Trushina, O. I.; Novikova, E. G.; Sokolov, V. V.; Filonenko, E. V.; Chissov, V. I.; Vorozhtsov, G. N. *Photodiagn Photodyn* **2008**, *5*, 256.
- (31) Jori, G.; Brown, S. B. *Photochem Photobiol Sci* **2004**, *3*, 403.
- (32) Maisch, T.; Szeimies, R. M.; Jori, G.; Abels, C. *Photochem Photobiol Sci* **2004**, *3*, 907.

- (33) Zeina, B.; Greenman, J.; Corry, D.; Purcell, W. M. *Br J Dermatol* **2002**, *146*, 568.
- (34) Lyon, J. P.; Azevedo, C. D. P. E.; Moreira, L. M.; de Lima, C. J.; de Resende, M. A. *Mycopathologia* **2011**, *172*, 293.
- (35) Dougherty, T. J.; Gomer, C. J.; Henderson, B. W.; Jori, G.; Kessel, D.; Korbelik, M.; Moan, J.; Peng, Q. *J Natl Cancer I* **1998**, *90*, 889.
- (36) Kalka, K.; Merk, H.; Mukhtar, H. *J Am Acad Dermatol* **2000**, *42*, 389.
- (37) De Rosa, F. S.; Bentley, M. V. L. B. *Pharmaceut Res* **2000**, *17*, 1447.
- (38) Szacilowski, K.; Macyk, W.; Drzewiecka-Matuszek, A.; Brindell, M.; Stochel, G. *Chem Rev* **2005**, *105*, 2647.
- (39) Donnelly, R. F.; McCarron, P. A.; Tunney, M. M. *Microbiol Res* **2008**, *163*, 1.
- (40) Demidova, T. N.; Hamblin, M. R. *Appl Environ Microbiol* **2005**, *71*, 6918.
- (41) Caruso, E.; Banfi, S.; Barbieri, P.; Leva, B.; Orlandi, V. T. *J Photoch Photobio B* **2012**, *114*, 44.
- (42) Kamkaew, A.; Lim, S. H.; Lee, H. B.; Kiew, L. V.; Chung, L. Y.; Burgess, K. *Chem Soc Rev* **2013**, *42*, 77.
- (43) He, H.; Lo, P. C.; Yeung, S. L.; Fong, W. P.; Ng, D. K. *Chem Commun* **2011**, *47*, 4748.
- (44) Kamkaew, A.; Burgess, K. *J Med Chem* **2013**, *56*, 7608.
- (45) Engelhardt, V.; Krammer, B.; Plaetzer, K. *Photochem Photobiol Sci* **2010**, *9*, 365.
- (46) Tanaka, M.; Kinoshita, M.; Yoshihara, Y.; Shinomiya, N.; Seki, S.; Nemoto, K.; Hamblin, M. R.; Morimoto, Y. *Laser Surg Med* **2011**, *43*, 221.
- (47) Lambrechts, S. A.; Demidova, T. N.; Aalders, M. C.; Hasan, T.; Hamblin, M. R. *Photoch Photobio Sci* **2005**, *4*, 503.
- (48) Navarre, W. W.; Schneewind, O. *Microbiol Mol Biol Rev* **1999**, *63*, 174.
- (49) Mutharia, L. M.; Crockford, G.; Bogard, W. C., Jr.; Hancock, R. E. *Infect Immun* **1984**, *45*, 631.

- (50) de Souza, S. C.; Junqueira, J. C.; Balducci, I.; Koga-Ito, C. Y.; Munin, E.; Jorge, A. O. *J Photochem Photobiol B* **2006**, *83*, 34.
- (51) Teichert, M. C.; Jones, J. W.; Usacheva, M. N.; Biel, M. A. *Oral Surg Oral Med Oral Pathol Oral Radiol Endod* **2002**, *93*, 155.
- (52) Costa, A. C. B. P.; Rasteiro, V. M. D.; Pereira, C. A.; Hashimoto, E. S. H. D.; Beltrame, M.; Junqueira, J. C.; Jorge, A. O. C. *Arch Oral Biol* **2011**, *56*, 1299.
- (53) Dovigo, L. N.; Pavarina, A. C.; Mima, E. G.; Giampaolo, E. T.; Vergani, C. E.; Bagnato, V. S. *Mycoses* **2011**, *54*, 123.
- (54) Cormick, M. P.; Quiroga, E. D.; Bertolotti, S. G.; Alvarez, M. G.; Durantini, E. N. *Photoch Photobio Sci* **2011**, *10*, 1556.
- (55) Lambrechts, S. A. G.; Aalders, M. C. G.; Van Marle, J. *Antimicrob Agents Chemother* **2005**, *49*, 2026.

CHAPTER 2

Survey of photosensitizer structure-activity relationships for *in vitro* photodynamic therapy of pathogenic yeast

2.1 Abstract

Opportunistic pathogenic yeast strains, such as those belonging to the genera *Candida* and *Cryptococcus*, can cause life-threatening infections in immunocompromised individuals. The improper use of antibiotics has increased the number of drug resistant bacterial strains, but the increase of fungal drug resistance has also raised the interest of searching for new alternative antimicrobial treatments. Herein, we performed *in vitro* antimicrobial photodynamic inactivation (aPDI) studies against *Candida albicans*, *Candida glabrata*, and *Cryptococcus neoformans* to survey the structure-activity relationships of photosensitizers for potential use in antifungal applications. Nine photosensitizers were studied: 5,10,15,20-tetrakis(1-methyl-4-pyrid-4-yl)porphyrin tetratosylate (TMPyP), 5,10,15,20-tetrakis(4-N,N,N-trimethylanilinium)porphyrin tetrachloride (TMNAP), 5,10,15,20-tetrakis(4-sulphonatophenyl)porphyrin (TSPP), 5,10,15,20-tetrakis(4-carboxyphenyl)porphyrin-Pd(II) (TCPP-Pd), methylene blue (MB), rose bengal (RB), 2,6-diiodo-1,3,5,7-tetramethyl-8-(N-methyl-4-pyridyl)-4,4' difluoroboradiazaindacene (JB461, BODIPY), 3,13-Dicarboxy-8,8,18,18-tetramethylbacteriochlorin (B23), and phthalocyanine tetrasulphonic acid (PhCS). The experimental design enabled the aPDI studies to investigate the photofungicidal efficiency in a concentration and light dose dependent manner. Overall, the results demonstrate that aPDT can exhibit broad spectrum antifungal activity when the

photosensitizers possess attributes that include i) a high quantum yield for singlet oxygen production, and ii) ionic character that enables a high solubility in water and allows for electrostatic interactions with the cells.

2.2 Introduction

Over the past decade, there has been a significant increase in the incidence rates of invasive fungal infections, especially for people with defective immune systems.^{1,2} Immunocompromised individuals, such as patients with acquired immunodeficiency syndrome (HIV/AIDS), chemotherapy patients, and those who have undergone surgeries or organ transplants, are prone to life-threatening opportunistic fungal infections that are caused by either endogenous systemic pathogens (*Candida* infections), or environmental pathogens through inhalation (*Cryptococcus* and *Aspergillus* infections).³⁻⁸ A common *Candida* infection is Candidemia, which is the fourth leading cause of bloodstream infection in the United States.⁹⁻¹³ Candidemia is problematic to patients in an intensive care unit (ICU) environment and is associated with a mortality rate of 30-70% depending on the age group.¹⁴⁻¹⁷ Cryptococcosis, a *Cryptococcus* infection caused by the encapsulated *C. neoformans*, is one of the most common life-threatening fungal infections, and is the leading cause of death for HIV/AIDS patients.³ There are an estimated 1 million cases of *C. neoformans* meningitis infection that occur annually, leading to nearly 625,000 deaths per year worldwide, a large number of which are concentrated in sub-Saharan Africa where co-infection with HIV/AIDS is particularly high.^{1,18}

Based upon previous studies, antimicrobial photodynamic inactivation (aPDI) may be one such alternative method for the treatment of fungal infections.²⁴⁻³² Demidova and Hamblin showed photoinactivation of 4 log units in CFU reduction for 200 μM of RB against *C. albicans* upon illumination.²⁷ Cormick *et al.* demonstrated 5 log units decrease of cell survival for *C. albicans* when incubated with 5 μM of tetracationic and tricationic porphyrin photosensitizers upon illumination with visible light.³³ Friedberg *et al.* performed *in vitro* PDT with 31.5 mg/L Green 2W against *Aspergillus fumigatus* and observed complete killing of the pathogen (2.7×10^6 CFU/mL) with a light dose of 385 J/cm².³⁴ Outside of these studies, however, there is a lack of understanding of the structure-activity relationships that govern photosensitizer efficacy in antifungal applications. Here we studied the aPDI susceptibility of three pathogenic yeast strains *in vitro* toward photosensitizers of different sizes, charges, and photophysical properties. Photodynamic efficacy was examined in a light dose and concentration dependent manner. The motivation for this study was to expand our knowledge of antifungal PDT to provide a foundation for future photosensitizer development.

2.3 Materials and Methods

Materials. Buffer salts were purchased from Fisher Scientific. Yeast peptone dextrose broth (YPD) and Sabouraud dextrose (SD) broth were obtained from BD Difco. Unless otherwise specified, all other chemicals were obtained from commercial sources in the highest purity available. Ultrapure water used for all media and buffers was provided by an Easypure II system (Barnstead). UV-visible absorption measurements were performed on a

Varian Cary 50 Bio, or a Genesys 10 UV scanning spectrophotometer from Thermo Electron Corp for single wavelength measurements.

Photosensitizers. Rose bengal (RB) was purchased from Sigma Aldrich (St. Louis, MO), methylene blue (MB) from Fischer Scientific (Fair Lawn, NJ), and 5,10,15,20-tetrakis(1-methyl-4-pyrid-4-yl)porphyrin tetratosylate (TMPyP), 5,10,15,20-tetrakis(4-N,N,N-trimethylanilinium)porphyrin tetrachloride (TMNAP), 5,10,15,20-tetrakis(4-sulphonatophenyl)porphyrin (TSPP), 5,10,15,20-tetrakis(4-carboxyphenyl)porphyrin-Pd(II) (TCPP-Pd), and phthalocyanine tetrasulphonic acid (PhCS) were purchased from Frontier Scientific (Logan, Utah). 3,13-Dicarboxy-8,8,18,18-tetramethylbacteriochlorin (B23) and 2,6-diiodo-1,3,5,7-tetramethyl-8-(N-methyl-4-pyridyl)-4,4'-difluoroboradiazaindacene (JB461, BODIPY) were kindly provided by Dr. Jonathan S. Lindsey and Dr. Walter W. Weare, respectively, from North Carolina State University. The stock solutions were prepared in water, DMSO (for B23), or in water/acetone (10% v/v) for TCPP-Pd. The chemical structures of all photosensitizers are shown in Figure 2.2 and their molecular and photophysical properties are listed in Table 2.1.

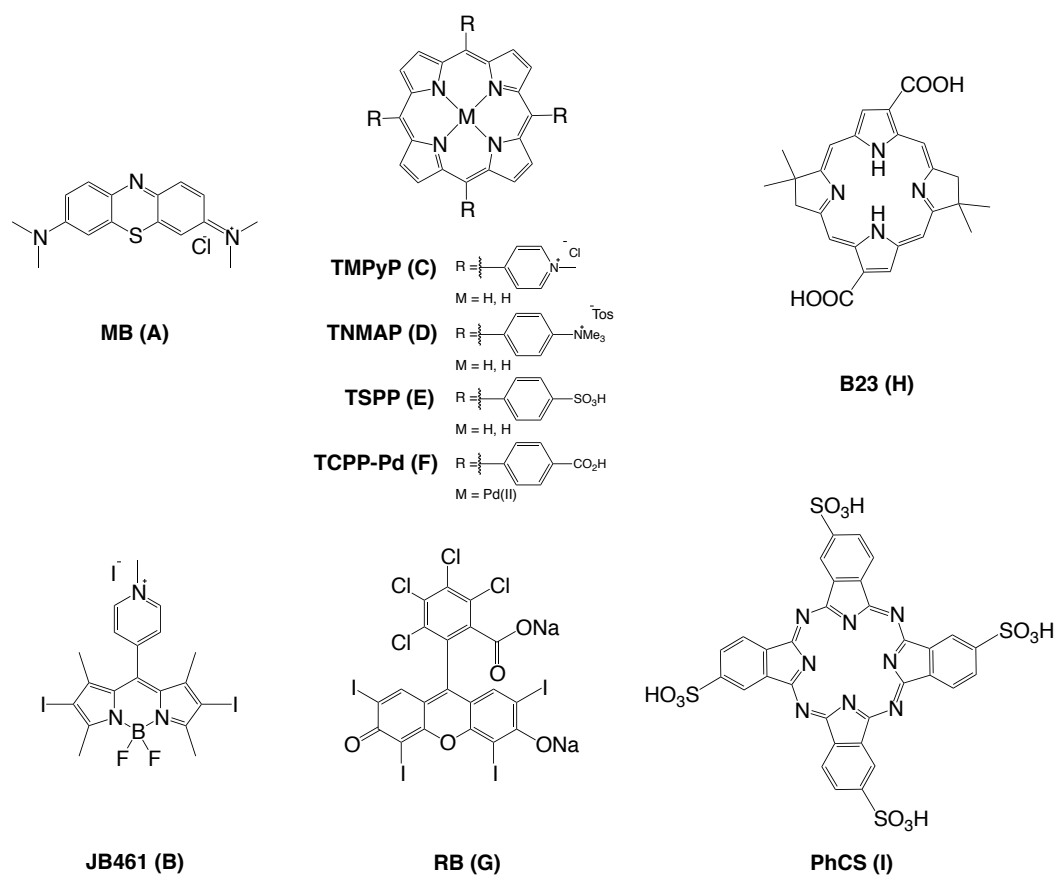


Figure 2.2. Chemical structures of photosensitizers employed in this study.

Table 2.1. Selected properties of the photosensitizers that affect PDT activity.

Photosensitizer	Number of charges	λ_{\max} (nm)	ϵ ($M^{-1} \text{ cm}^{-1}$)	$\Phi^1\text{O}_2$	Reference
MB (A)	+1	660	95,000	0.49 (EtOH)	35
JB461 (B)	+1	546	110,000	N/A	36
TMPyP (C)	+4	424	194,000	0.74 (PBS)	37
TMNAP (D)	+4	412	178,144	0.48 (PBS)	37
TSPP (E)	-4	410	163,000	0.75 (PBS)	37
TCPP-Pd (F)	-4	416	N/A	0.53 (PBS)	35
RB (G)	-2	540	89,000	0.75 (PBS)	35
B23 (H)	-2	748	N/A	N/A	38
PhCS (I)	-1	702	99,800	0.14 (H ₂ O)	37

λ_{\max} = Absorption maximum

ϵ = Molar absorptivity

$\Phi^1\text{O}_2$ = Quantum yield of singlet oxygen production

Cell Culture. *Candida albicans* (ATCC 90028), *Candida glabrata* (ATCC 15545), and *Cryptococcus neoformans* (ATCC 64538) were obtained from the American Type Culture Collection (ATCC, Manassas, VA). *C. albicans* and *C. glabrata* were inoculated in YPD broth and incubated overnight at 37°C. *C. neoformans* were inoculated in SD broth at 30°C for 48 hr.

Incubation of Cells with Photosensitizers. Each culture was pelleted by centrifugation (10 min, ~3700 x g) at 4 °C, and washed twice with sequential resuspension in phosphate buffer saline (PBS: 170 mM NaCl, 3.4 mM KCl, 10.0 mM Na₂HPO₄, 1.8 mM KH₂PO₄, pH 7.2) followed by centrifugation to remove excess media. Then the cells were diluted in PBS to a cell concentration of ~2.0x10⁷ colony forming units (CFU) per mL as determined by spectrophotometry at 600 nm (OD₆₀₀). From a 5 mL volume of cell culture, a 1 mL aliquot was transferred to a separate culture tube to serve as a compound-free control. To the remaining 4 mL culture was added an appropriate volume of the photosensitizer (PS) stock solution to give the final desired PS concentration. The 4 mL culture was incubated in the presence of the photosensitizer on an orbital shaker in the dark for 30 minutes.

Antimicrobial Photodynamic Therapy Assay. All photosensitization experiments were performed using a non-coherent light source, PDT light model LC122 (LumaCare, USA), and the fluence was measured with an Orion power meter (Orphir Optronics Ltd, Israel). After incubation, three 1 mL aliquots of the cell suspension were transferred to a sterile 24-well plate (BD Falcon, flat bottom) and illuminated with visible light (400 - 700 nm) with a fluence of 65±5 mW/cm² for 15 or 30 min while magnetically stirred. The remaining 1 mL culture was kept in the absence of light (as the dark control).

After illumination, each well was 1:10 serially diluted five times. 10 μ L from the undiluted well and from each dilution, as well as from the compound-free control and dark control, were plated and incubated in the dark at 37°C. Each strain was grown on gridded six column square agar plates made with their respective growth media. The survival rate was determined from the ratio of CFU/mL of the illuminated solution versus that of the compound-free control. The detection limit was set to 0.01-0.001%. Samples with PS present but kept in the dark (dark control) and samples without PS but kept in the dark (PS-free control) were served as controls. All experiments were conducted in triplicate at a minimum, and statistical significance was assessed via a two-tailed, unpaired Student's t-test.

2.4 Results and discussion

Photodynamic efficacy is related to the photophysical and chemical behavior of the photosensitizer, as well as the biological structure and function of the targeted cell components. In order to evaluate the role of size, charge, and singlet oxygen production of the photosensitizers on aPDI efficacy, a series of photosensitizers were investigated for their antimicrobial photodynamic properties against the following fungal pathogens: *C. albicans*, *C. glabrata* and *C. neoformans*. The studies were also performed as a function of light dose and photosensitizer concentration. In all experiments, yeast cells were incubated with the PS for 30 mins, then illuminated at 65 ± 5 mW/cm² for either 15 or 30 min, which corresponds to a total fluence of 59 or 118 J/cm². Cell survival was calculated from the ratio between cells with PS and light treatment versus the dark, PS-free control (the latter set to 100% survival). In the control experiments, cells treated with light in the absence of the PS, and cells treated

with the PS but in the absence of light, showed little or no CFU difference compare to the dark control (no compound and no light). On the other hand, different degrees of cell inactivation efficacy were observed between PS of different charges (cationic and anionic) and sensitizers of different sizes (vide infra).

2.4.1 Photoinactivation of cationic photosensitizers

Methylene blue showed no photoinactivation at lower PS concentrations for the *Candida* species. However, with a 10 fold increase in concentration (10 μ M), MB exhibited a \sim 4 log unit CFU reduction with 30 min of light exposure for *C. albicans* (Fig. 2.4A) and *C. glabrata* (Fig. 2.5A). *C. neoformans* showed similar photofungicidal activity with only 1 μ M of MB and 30 min illumination (Fig. 2.6A). We surmise that methylene blue is more effective for *C. neoformans* than the *Candida* species likely due to more favorable PS charge/cell wall charge interactions. *Candida* cells contain a cell membrane that is relatively neutral, which likely reduces the interaction between the cationic MB, when compared to the anionic cell membrane of *C. neoformans*. Also, *Candida* cells are almost double in size (10-12 microns) compared to *C. neoformans* (\sim 2.5 microns without capsule),³⁹ and thus may require more PS molecules to bind to the cell for effective photodynamic inactivation.

All three fungal strains were highly susceptible to JB461-mediated aPDI. In fact, JB461 (BODIPY) exhibited the greatest degree of photoinactivation amongst the four cationic PS tested for all three fungal strains. The PDI of *C. albicans* was examined using different BODIPY concentrations and illumination times (Fig. 2.4B). After 15 min of light treatment with 100 nM to 1 μ M of the photosensitizer, no inactivation was observed.

However, as we increased the illumination time to 30 min, cell inactivation reached 99.999% at 1 μ M. *C. glabrata*, another strain of Candida species, was also investigated (Fig. 2.5B). *C. glabrata* was slightly less susceptible to JB461 compared to *C. albicans*. Under the same photodynamic condition mentioned above, 3 logs of CFU reduction was achieved that is 2 logs difference compared to *C. albicans*. The viability of *C. neoformans* after 15 min illumination depended on the concentration of the BODIPY PS (Fig. 2.6B): after treatment with 100 or 500 nM of sensitizer, *C. neoformans* was able to achieve only 1 log unit of inactivation. However, photoinactivation was enhanced to a 5 log unit CFU reduction as the sensitizer concentration increased to 1 μ M. When illuminated for 30 minutes in the presence of 500 nM of JB461, *C. neoformans* exhibited a detection limit 5 log unit CFU reduction, and was the most effective PS towards *C. neoformans* inactivation. To the best of our knowledge, there are no previous literature precedents using BODIPY-based compounds as photosensitizers for the inactivation of pathogenic fungal species.

Both tetra-cationic porphyrins, TMPyP (Figs. 2.4-2.6C) and TMNAP (Figs. 2.4-2.6D), showed comparable photoinactivation against *C. glabrata* and *C. albicans*. Both Candida strains showed a \sim 4 log unit CFU reduction when incubated with 1 μ M PS and 30 min of light illumination for TMPyP (Fig. 2.3C and 2.4C), and were equivalently less susceptible when TMNAP (2 logs CFU reduction) was employed as the PS under the same conditions (Fig. 2.4D and 2.5D). TMPyP and TMNAP were slightly less effective against *C. neoformans*: a 3 log unit and a 1 log unit CFU reduction, respectively, were observed (Fig. 2.6C and 2.6D). The difference in phototoxicity between TMPyP and TMNAP may be explained by their singlet oxygen production quantum yield, which are 0.75 and \sim 0.5,

respectively. The Φ_{Δ} for TMPyP is higher than TMNAP, and will therefore produce more reactive oxygen species for cell inactivation under the same photodynamic conditions.

C. neoformans was found to be much more susceptible to the BODIPY PS when compared with the cationic porphyrins. Two possible explanations can account for this: i) the BODIPY compound is much smaller in size compared to TMPyP and TMNAP, which enabled it to possibly localize deeper into the cell membrane, and leading to the observed increase in photoinactivation; ii) it is possible that the BODIPY PS has a higher singlet oxygen quantum yield. However, as this value for JB461 is not available, we cannot compare its singlet oxygen efficacy to other photosensitizers and conclude whether JB461 is more favorable in singlet oxygen production or not.

Overall, the degree of photoinactivation for *C. glabrata* was found to be slightly less than that observed for *C. albicans* for all PS tested in this study, suggesting that *C. glabrata* may be more resistant to PDT treatment than *C. albicans*. The difference in photoinactivation efficacy between the three different yeast strains may be attributed to differences in their extracellular structures. *C. neoformans* is encapsulated and known to produce melanin, while *Candida* species do not. The capsule contains highly negative charged polysaccharides found right outside the cell wall,⁴⁰⁻⁴² namely, glucuronoxylomannan (GXM) and galactoxylomannan (GalXM) and mannoprotein (Fig. 2.3) where GXM makes up approximately 90% of the capsule composition and range from 1 to 50 μm .³⁹ Both the polysaccharide and melanin production are responsible for the strong negative charge on the cell surface. The high PDI efficacy of the cationic BODIPY PS towards *C. neoformans* may

be explained by a strong electrostatic interaction between the cell surface and the photosensitizer.

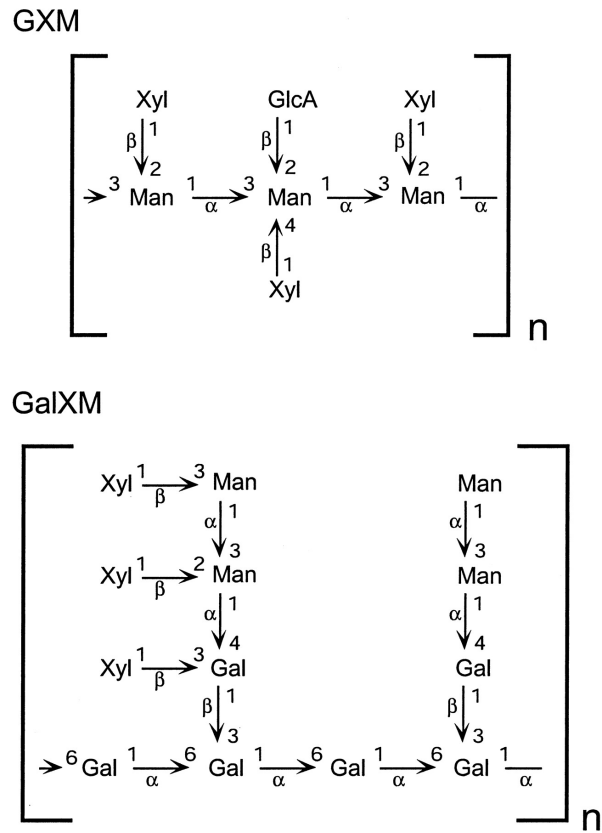


Figure. 2.3. Structures of cryptococcal capsular polysaccharides, glucuronoxylomannan (GXM) and galactoxylomannan (GalXM). Adapted from Bar-Peled *et al.*⁴¹

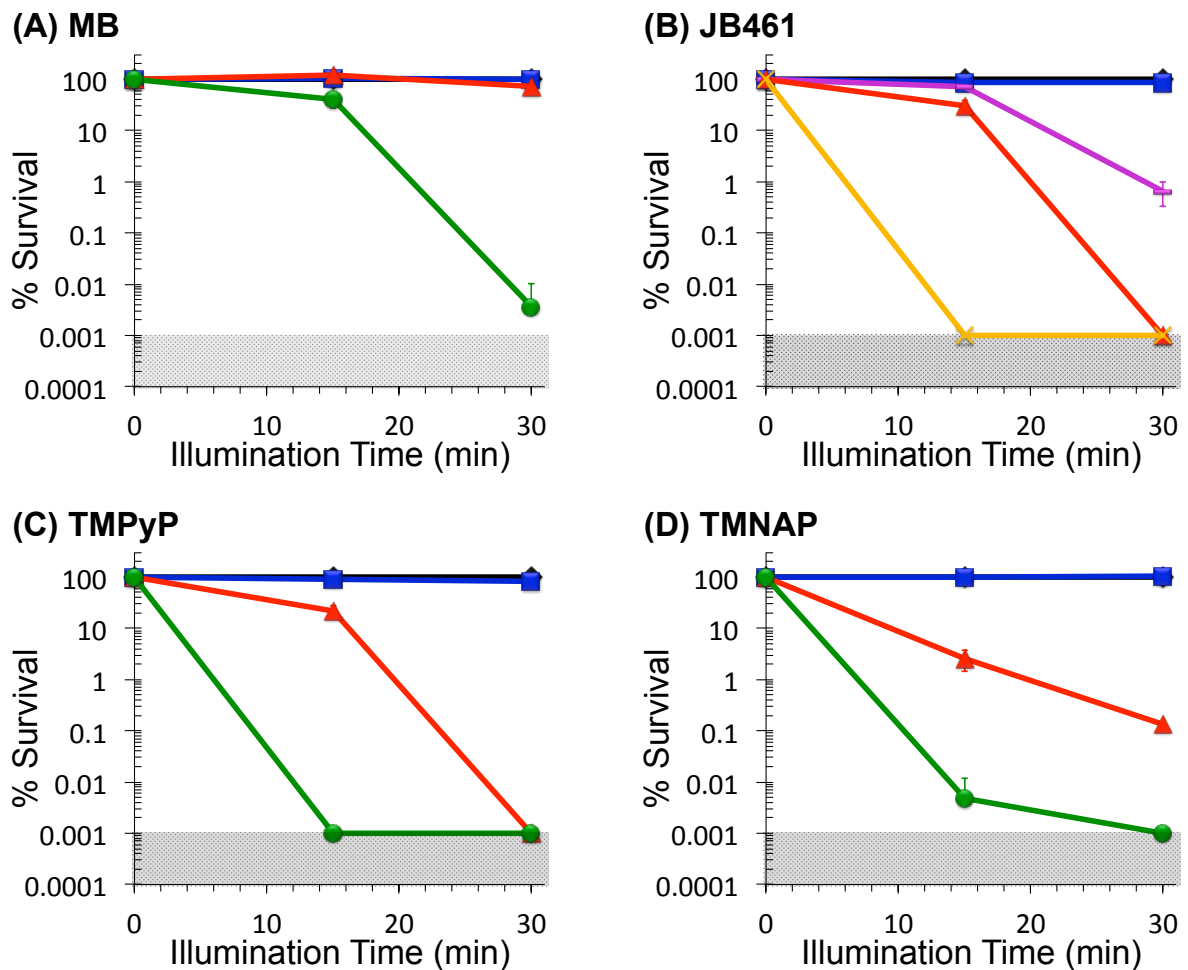


Figure 2.4. Photoinactivation of *Candida albicans*. Cultures of *C. albicans* were incubated in the dark with cationic photosensitizers (A) MB, (B) JB461, (C) TMPyP, (D) TMNAP, for 30 min at 37°C and illuminated with white light (400-700nm) for 15 and 30 min at a fluence of $65 \pm 5 \text{ mW/cm}^2$: PS-free, dark control (◆), 100 nM (■), 500 nM (-), 1 μM (▲), 5 μM (×), and 10 μM (●). The detection limit was set to 0.001% survival.

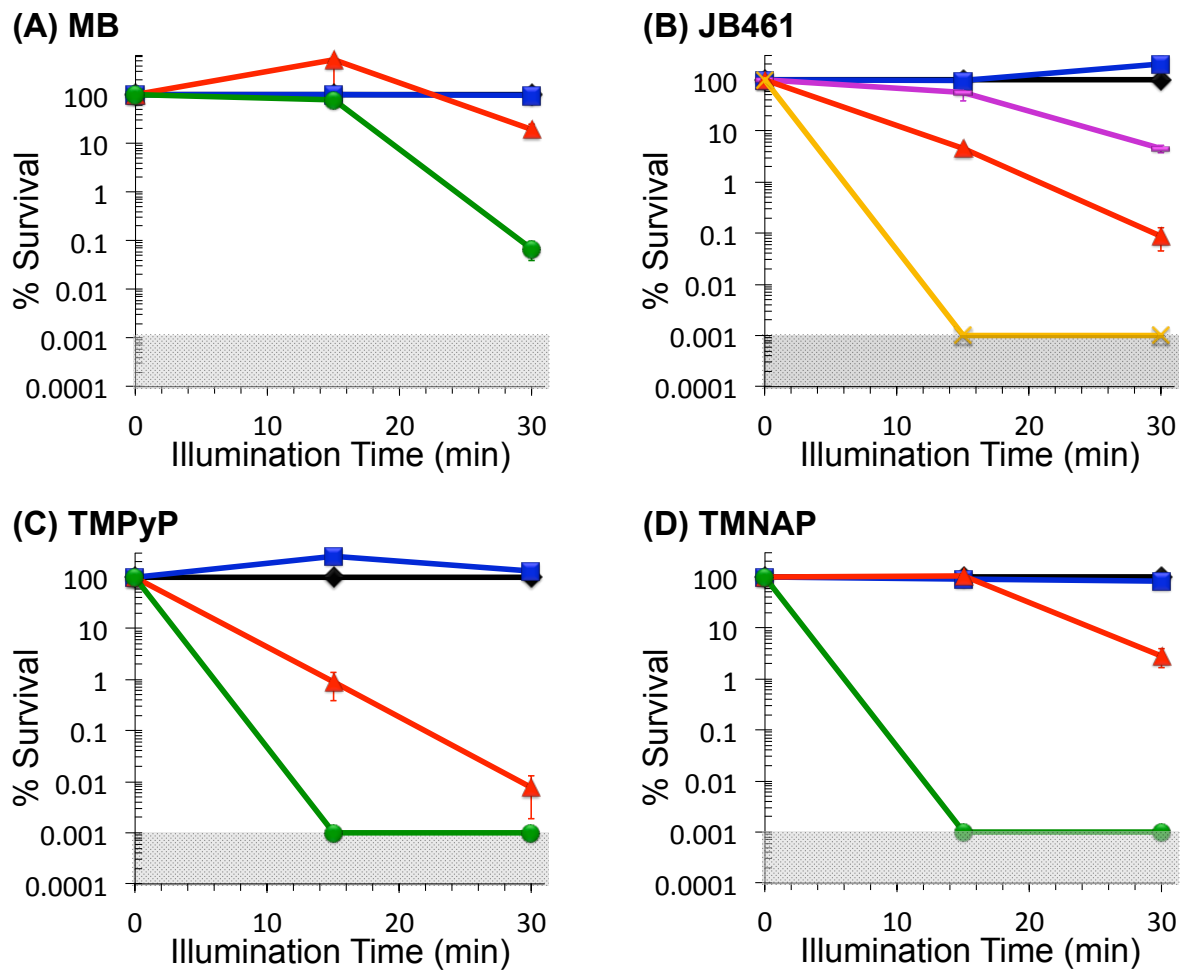


Figure 2.5. Photoinactivation of *Candida glabrata*. Cultures of *C. glabrata* were incubated in the dark with cationic photosensitizers (A) MB, (B) JB461, (C) TMPyP, (D) TMNAP, for 30 min at 37°C and illuminated with white light (400-700nm) for 15 and 30 min at a fluence of $65 \pm 5 \text{ mW/cm}^2$: PS-free, dark control (◆), 100 nM (■), 500 nM (-), 1 μM (▲), 5 μM (×), and 10 μM (●). The detection limit was set to 0.001% survival.

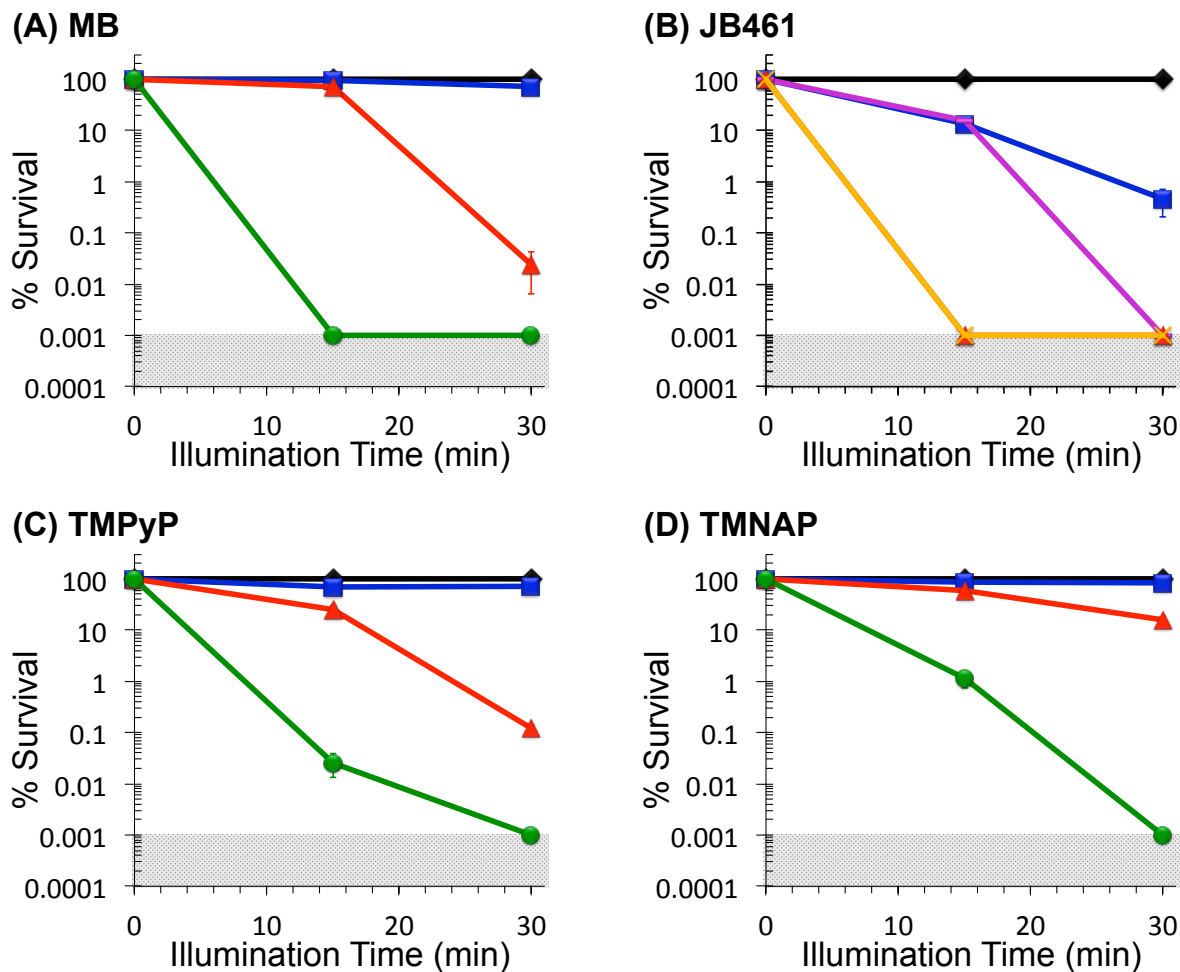


Figure 2.6. Photoinactivation of *Cryptococcus neoformans*. Cultures of *C. neoformans* were incubated in the dark with cationic photosensitizers (A) MB, (B) JB461, (C) TMPyP, (D) TMNAP, for 30 min at 37°C and illuminated with white light (400-700nm) for 15 and 30 min at a fluence of $65 \pm 5 \text{ mW/cm}^2$: PS-free dark control (◆), 100 nM (■), 500 nM (-), 1 μM (▲), 5 μM (×), and 10 μM (●). The detection limit was set to 0.001% survival.

2.4.2 Photoinactivation of anionic photosensitizers

The two *Candida* strains exhibited similar photoinactivation susceptibility towards anionic photosensitizers. The anionic porphyrins (TSPP (E) and TCPP-Pd (F)) were most effective amongst the five anionic sensitizers tested against *C. albicans* (Fig 2.7E and 2.7F)

and *C. glabrata* (Fig 2.8E and 2.8F), with detection limit (>99.999%) photoinactivation observed for both strains under the aPDI conditions of 1 μ M with 15 min light illumination. Even at a lower PS concentration of 0.1 μ M with 30 min illumination, a 2-3 log unit CFU reduction was observed. TSPP has a quantum yield (Φ_{Δ}) of singlet oxygen production of \sim 0.75, which is equivalent to the cationic porphyrin TMPyP (0.74), but greater than that of TMNAP (\sim 0.5). RB ($\Phi_{\Delta} = 0.75$) only showed photoactivity at the highest concentrations examined (>99.999%, 10 μ M, 15 min illumination) for both *Candida* species (Fig. 2.7G & 2.8G).

The photoactivity of the anionic bacteriochlorin, B23, was very limited: at a high concentration of 10 μ M and with 30 min illumination, a maximum 3 log unit CFU reduction was observed for both *Candida* strains (Fig. 2.7H & 2.8H), and a 1 log CFU reduction was observed for *C. neoformans* (Fig. 2.9H). PhCS displayed no photoactivity towards all three fungal strains, even at high PS concentration and long illumination times. (Fig. 2.7I to 2.9I) This is possibly due to 1) the quantum yields for PhCS ($\Phi_{\Delta} = 0.14$) is relatively unfavorable for singlet oxygen production when compared with the other PS employed in this study, and which therefore led to limited or no cytotoxicity being observed, or 2) the binding affinities for this anionic PS was very low, which is not sufficient to produce singlet oxygen in close enough proximity of the cell to lead to cell damage.

The *C. neoformans* cell wall is strongly anionic in nature, making it difficult for anionic PS to localize into the cell membrane.^{41,42,44} This leads to a proximity effect wherein the singlet oxygen generated is not localized at the cell. Amongst the five anionic photosensitizers, RB was the only one that showed photoactivity against *C. neoformans* (Fig

2.9G), with a 2 log unit CFU reduction being observed at 1 μM PS for 30 min illumination, and >99.999% cell death at 10 μM PS with 15 min illumination. The quantum yield (Φ_{Δ}) of singlet oxygen production for RB is 0.75, which is similar to TSPP \sim 0.75. As the level of phototoxicity is different between the two, this suggests that the size of the PS (possibly as charge density) may also play a key role in cell penetration.

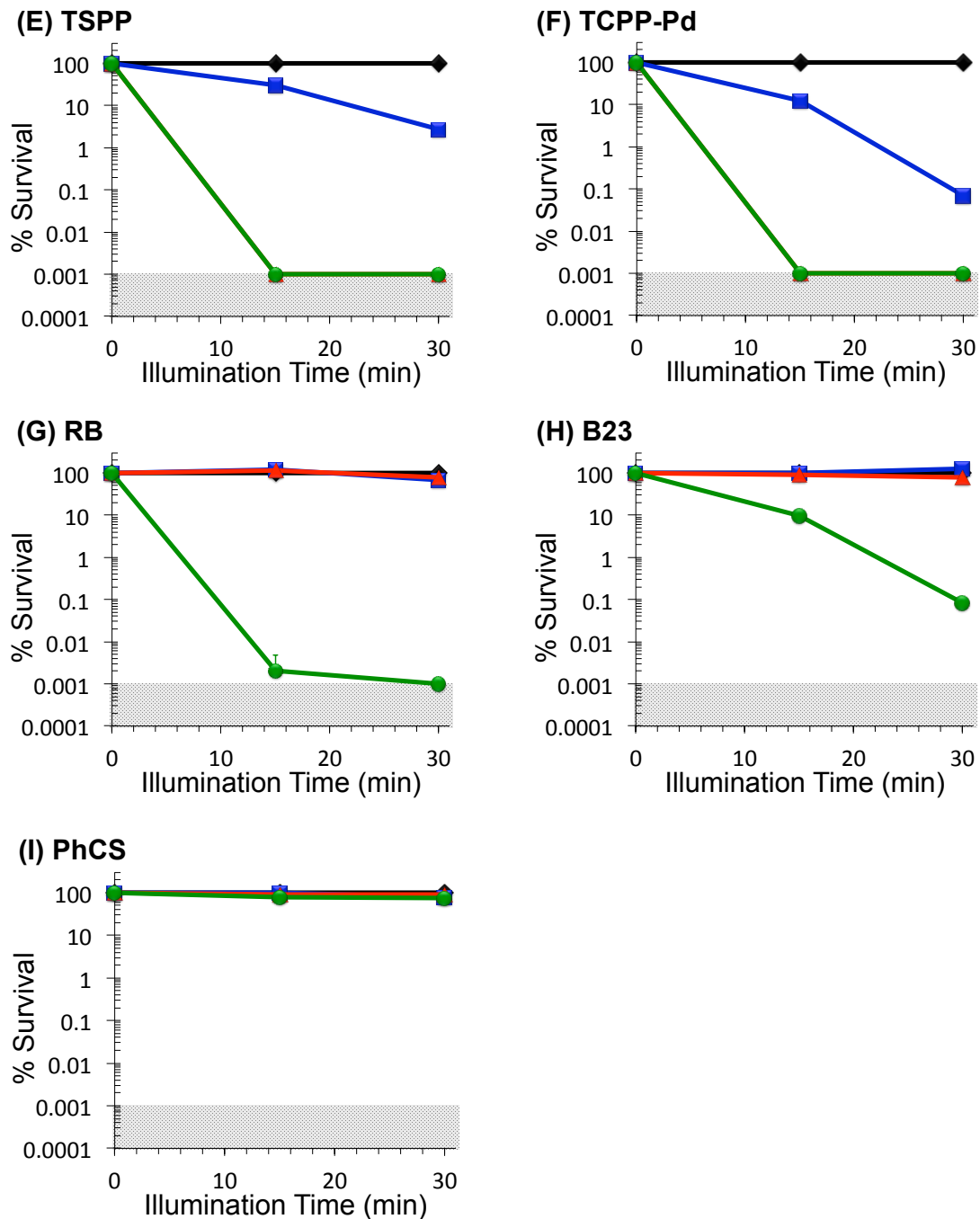


Figure 2.7. Photoinactivation of *Candida albicans*. Cultures of *C. albicans* were incubated in the dark with anionic photosensitizers (E) TSPP, (F) TCPP-Pd, (G) RB, (H) B23, (I) PhCS for 30 min at 37°C and illuminated with white light (400-700nm) for 15 and 30 min at a fluence of $65 \pm 5 \text{ mW/cm}^2$: PS-free, dark control (◆), 100 nM (■), 1 μM (▲), and 10 μM (●). The detection limit was set to 0.001% survival.

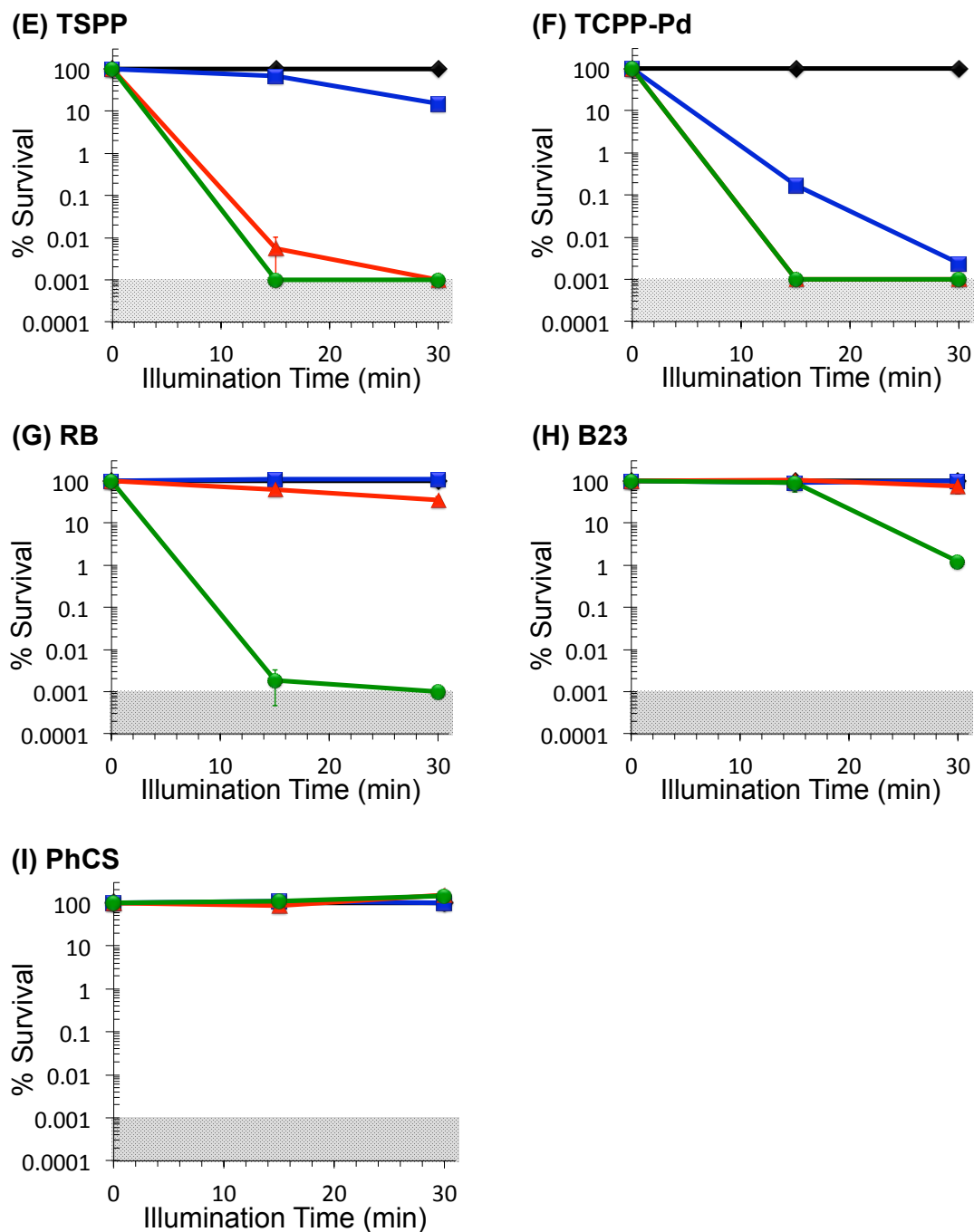


Figure 2.8. Photoinactivation of *Candida glabrata*. *C. glabrata* were incubated in the dark with anionic photosensitizers (E) TSPP, (F) TCPP-Pd, (G) RB, (H) B23, (I) PhCS for 30 min at 37°C and illuminated with white light (400-700nm) for 15 and 30 min at a fluence of 65 ± 5 mW/cm²: PS-free, dark control (◆), 100 nM (■), 1 μM (▲), and 10 μM (●). The detection limit was set to 0.001% survival.

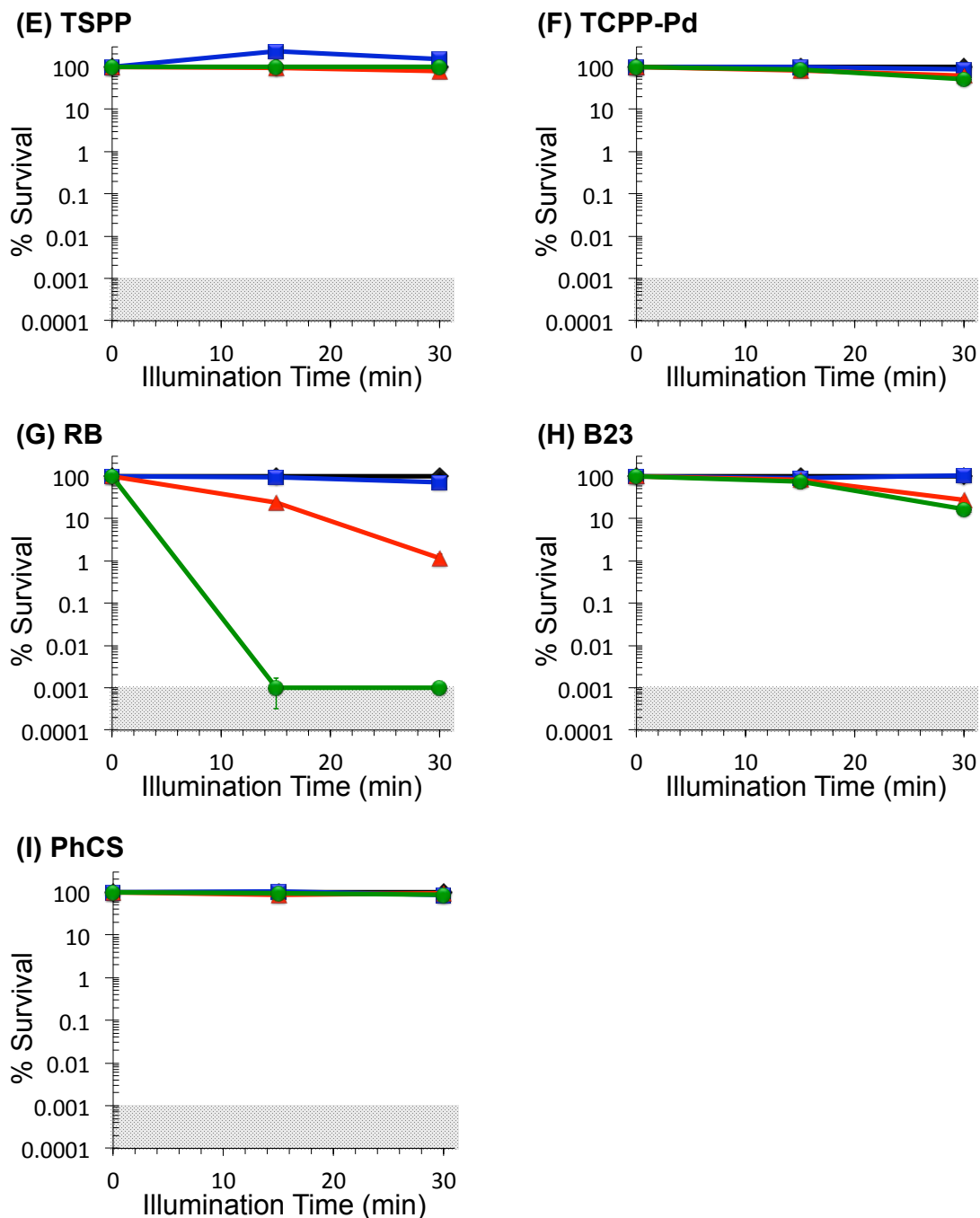


Figure 2.9. Photoinactivation of *Cryptococcus neoformans*. *C. neoformans* were incubated in the dark with anionic photosensitizers (E) TSPP, (F) TCPP-Pd, (G) RB, (H) B23, (I) PhCS for 30 min at 37°C and illuminated with white light (400-700nm) for 15 and 30 min at a fluence of $65 \pm 5 \text{ mW/cm}^2$: PS-free, dark control (◆), 100 nM (■), 1 μM (▲), and 10 μM (●). The detection limit was set to 0.001% survival.

2.5 Conclusions

We have demonstrated the aPDI activity of a range of photosensitizers of different sizes and charges at various concentrations and light doses against three strains of pathogenic fungus. Promising results were obtained for both cationic and anionic photosensitizers. For the *Candida* and *Cryptococcus* strains examined, detection limit photoinactivation was obtained at a concentration of 1 μM and 500 nM, respectively, for JB461. All three pathogens were susceptible to cationic porphyrins at various concentrations. Anionic porphyrins were able to photoinactivate both *Candida* strains at 1 μM . However, due to its negatively charged cell membrane, *C. neoformans* was not susceptible to most anionic PS, with the exception of Rose Bengal. Anionic bacteriochlorin (B23) also showed 2-3 log units CFU reduction at 10 μM for all three pathogens, and the anionic phthalocyanine showed no killing for all 3 fungal strains. These results provide a foundation for future photosensitizer development and PS-conjugate tuning.

REFERENCES

- (1) McNeil, M. M.; Nash, S. L.; Hajjeh, R. A.; Phelan, M. A.; Conn, L. A.; Plikaytis, B. D.; Warnock, D. W. *Clin Infect Dis* **2001**, *33*, 641.
- (2) Beck-Sague, C.; Jarvis, W. R. *J Infect Dis* **1993**, *167*, 1247.
- (3) Mitchell, T. G.; Perfect, J. R. *Clin Microbiol Rev* **1995**, *8*, 515.
- (4) Currie, B. P.; Casadevall, A. *Clin Infect Dis* **1994**, *19*, 1029.
- (5) Klevens, R. M.; Edwards, J. R.; Richards, C. L., Jr.; Horan, T. C.; Gaynes, R. P.; Pollock, D. A.; Cardo, D. M. *Public Health Rep* **2007**, *122*, 160.
- (6) Alangaden, G. J. *Infect Dis Clin North Am* **2011**, *25*, 201.
- (7) Bodey, G. P.; Vartivarian, S. *Eur J Clin Microbiol* **1989**, *8*, 413.
- (8) d'Enfert, C. *Curr Opin Microbiol* **2009**, *12*, 358.
- (9) Wisplinghoff, H.; Bischoff, T.; Tallent, S.; Seifert, H.; Wenzel, R.; Edmond, M. *Clin Infect Dis* **2004**, *39*, 309
- (10) Edmond, M. B.; Wallace, S. E.; McClish, D. K.; Pfaller, M. A.; Jones, R. N.; Wenzel, R. P. *Clin Infect Dis* **1999**, *29*, 239.
- (11) Ammerlaan, H. S.; Harbarth, S.; Buiting, A. G.; Crook, D. W.; Fitzpatrick, F.; Hanberger, H.; Herwaldt, L. A.; van Keulen, P. H.; Kluytmans, J. A.; Kola, A.; Kuchenbecker, R. S.; Lingaas, E.; Meessen, N.; Morris-Downes, M. M.; Pottinger, J. M.; Rohner, P.; dos Santos, R. P.; Seifert, H.; Wisplinghoff, H.; Ziesing, S.; Walker, A. S.; Bonten, M. J. *Clin Infect Dis* **2013**, *56*, 798.
- (12) Almirante, B.; Rodriguez, D.; Cuenca-Estrella, M.; Almela, M.; Sanchez, F.; Ayats, J.; Alonso-Tarres, C.; Rodriguez-Tudela, J.; Pahissa, A. *J Clin Microbiol* **2006**, *44*, 1681
- (13) Rangel-Frausto, M.; Wiblin, T.; Blumberg, H.; Saiman, L.; Patterson, J.; Rinaldi, M.; Pfaller, M.; Edwards, J.; Jarvis, W.; Dawson, J.; Wenzel, R. *Clin Infect Dis* **1999**, *29*, 253
- (14) Wenzel, R. P. *Clin Infect Dis* **1995**, *20*, 1531.

- (15) Pittet, D.; Tarara, D.; Wenzel, R. P. *JAMA* **1994**, *271*, 1598.
- (16) Morrell, M.; Fraser, V.; Kollef, M. *Antimicrob Agents Chemother* **2005**, *49*, 3640
- (17) Bouza, E.; Munoz, P. *Int J Antimicrob Ag* **2008**, *32*, Supplement 2, S87.
- (18) Park, B. J.; Wannemuehler, K. A.; Marston, B. J.; Govender, N.; Pappas, P. G.; Chiller, T. M. *AIDS* **2009**, *23*, 525.
- (19) Espinel-Ingroff, A. In *Encyclopedia of Microbiology (Third Edition)*; Academic Press: Oxford, 2009, p 205.
- (20) Bell, A. S. In *Comprehensive Medicinal Chemistry II*; Elsevier: Oxford, 2007, p 445.
- (21) Kathiravan, M. K.; Salake, A. B.; Chothe, A. S.; Dudhe, P. B.; Watode, R. P.; Mukta, M. S.; Gadhwane, S. *Bioorg Med Chem* **2012**, *20*, 5678.
- (22) Masman, M. F.; Rodriguez, A. M.; Raimondi, M.; Zacchino, S. A.; Luiten, P. G. M.; Somlai, C.; Kortvelyesi, T.; Penke, B.; Enriz, R. D. *Eur J Med Chem* **2009**, *44*, 212.
- (23) Espinel-Ingroff, A. *Rev Iberoam Micol* **2009**, *26*, 15.
- (24) Demidova, T. N.; Hamblin, M. R. *Appl Environ Microbiol* **2005**, *71*, 6918.
- (25) Maisch, T.; Szeimies, R. M.; Jori, G.; Abels, C. *Photochem Photobiol Sci* **2004**, *3*, 907.
- (26) Bagnato, V. S.; Kurachi, C.; Ferreira, J.; Marcassa, L. G.; Sibata, C. H.; Allison, R. R. *Photodiagn Photodyn* **2005**, *2*, 107.
- (27) Demidova, T. N.; Hamblin, M. R. *Int J Immunopathol Pharmacol* **2004**, *17*, 245.
- (28) Demidova, T. N.; Hamblin, M. R. *Int J Immunopathol Pharmacol* **2004**, *17*, 117.
- (29) Hamblin, M. R.; Hasan, T. *Photochem Photobiol Sci* **2004**, *3*, 436.
- (30) Jori, G.; Brown, S. B. *Photochem Photobiol Sci* **2004**, *3*, 403.
- (31) Lyon, J. P.; Azevedo, C. D. P. E.; Moreira, L. M.; de Lima, C. J.; de Resende, M. A. *Mycopathologia* **2011**, *172*, 293.
- (32) Teichert, M. C.; Jones, J. W.; Usacheva, M. N.; Biel, M. A. *Oral Surg Oral Med Oral Pathol Oral Radiol Endod* **2002**, *93*, 155.

- (33) Cormick, M. P.; Quiroga, E. D.; Bertolotti, S. G.; Alvarez, M. G.; Durantini, E. N. *Photoch Photobio Sci* **2011**, *10*, 1556.
- (34) Friedberg, J. S.; Skema, C.; Baum, E. D.; Burdick, J.; Vinogradov, S. A.; Wilson, D. F.; Horan, A. D.; Nachamkin, I. *J Antimicrob Chemoth* **2001**, *48*, 105.
- (35) Redmond, R. W.; Gamlin, J. N. *Photochem Photobiol* **1999**, *70*, 391.
- (36) Caruso, E.; Banfi, S.; Barbieri, P.; Leva, B.; Orlandi, V. T. *J Photoch Photobio B* **2012**, *114*, 44.
- (37) Wilkinson, F.; Helman, W. P.; Ross, A. B. *J Phys Chem Ref Data* **1993**, *22*, 113.
- (38) Ruzie, C.; Krayner, M.; Balasubramanian, T.; Lindsey, J. S. *J Org Chem* **2008**, *73*, 5806.
- (39) Frases, S.; Pontes, B.; Nimrichter, L.; Rodrigues, M. L.; Viana, N. B.; Casadevall, A. *Biophys J* **2009**, *97*, 937.
- (40) McFadden, D.; Zaragoza, O.; Casadevall, A. *Trends Microbiol* **2006**, *14*, 497.
- (41) McFadden, D. C.; De Jesus, M.; Casadevall, A. *J Biol Chem* **2006**, *281*, 1868.
- (42) Zaragoza, O.; Rodrigues, M. L.; De Jesus, M.; Frases, S.; Dadachova, E.; Casadevall, A. *Adv Appl Microbiol* **2009**, *68*, 133.
- (43) Bar-Peled, M.; Griffith, C. L.; Doering, T. L. *Proc Natl Acad Sci U S A* **2001**, *98*, 12003.
- (44) Zaragoza, O.; Telzak, A.; Bryan, R. A.; Dadachova, E.; Casadevall, A. *Mol Microbiol* **2006**, *59*, 67.

CHAPTER 3

Cellulose nanocrystal-porphyrin conjugates and their antifungal properties

3.1 Abstract

Hospital acquired infections (HAI) are the sixth leading cause of death in the United States and affect nearly 2.5 million patients a year, especially those with compromised immune systems. Sterilized surfaces and patient-care equipment are key aspects to avoiding such infections. Materials that maintain a sterile surface over long durations, with minimal effort and without leading to drug-resistance, are needed to prevent surface transmission of pathogenic microbials. Two previously synthesized cellulose nanocrystal-porphyrin conjugates, CNC-CatPor and CNC-AnPor, that showed effective photoinactivation towards drug-resistant bacterial strains were used in this study to explore their photodynamic antifungal properties against two pathogenic fungal strains, *Candida albicans* and *Cryptococcus neoformans*. The photodynamic inactivation of *Candida albicans* with a suspension of CNC-CatPor, a material that is insoluble in aqueous solution, showed ~5 log units reduction of colony forming units (CFU) upon illumination with visible light (400-700 nm; 65 ± 5 mW/cm²) for 30 min. Studies on *Cryptococcus neoformans* achieved 1.5 logs of CFU reduction. CNC-AnPor was able to effectively inactivate *C. albicans* at 30 μ M with 30 min of light illumination (99.999%). While CNC-AnPor was anticipated to be completely inactive towards *C. neoformans* due to unfavorable electrostatic interactions with the negatively charged cell membrane of the fungus, CFU reduction was in fact observed for *C. neoformans* (4.5 logs) when incubated with 20 μ M of the material in the absence of light,

suggesting that CNC-AnPor itself may be antifungal even without a photodynamic application. The results suggest that cellulose-porphyrin conjugates may find utility as a potential antimicrobial material to prevent the transmission of fungal infections.

3.2 Introduction

Hospital-acquired infections (HAIs) are nosocomial infections caused by opportunistic bacteria or fungi in health care associated settings. According to the Centers for Disease Control and Prevention, in the United States alone nearly 2.5 million patients acquire an HAI annually, leading to 100,000 deaths each year, and now represent the sixth leading cause of death.¹ The microorganisms responsible for HAIs can be easily transmitted from surfaces as diverse as medical devices, counter tops, linens, and clothing. Incredibly, 1 in every 20 patients who are admitted into a hospital will contract an HAI.^{2,3} Patients with HAIs are more vulnerable for other infections, resulting in an increase in their mortality rate, lengthened hospital stays, and an increase in the associated health care cost. Patients diagnosed with an HAI have stays lengthened by an average of 24 days, and a cost increase of \$30,000 to \$40,000.⁴ Overall, HAIs cost the U.S. health care system about \$28-45 billion annually.

While combatting bacterial infections has been the focus of many efforts, fungal HAIs, often overlooked, also contribute significantly to the problem. Fungi belonging to the genus *Candida* are the fourth leading causative agent of HAIs, and are responsible for 90% of hospital-acquired fungal infections. Candidemia is the fourth leading cause of blood stream infections in the U.S., with a crude mortality rate of 50%.⁵⁻⁹ *Cryptococcus*

neoformans is the most common opportunistic infection for HIV-positive patients, with a mortality rate of 30%.^{10,11} Fungi such as *Candida albicans* can adhere on linens and gloves for up to 7 days. Moreover, fungal strains found in hospital environments are usually multi-drug resistant.¹² Thus, there is an urgent need for antifungal materials that prevent the surface transmission of pathogenic fungi in health care associated settings.

Most research efforts have focused on the development of antibacterial disinfectant materials, with little attention paid to antifungals. Materials currently being investigated as potential surface anti-infectives include antimicrobial polymeric materials containing quaternary ammonium¹³⁻¹⁶ and phosphonium salts,^{17,18} antifungal hydrogels,¹⁹ polyvinylchloride,²⁰⁻²² and antimicrobial films or hard surfaces coated with copper and titanium dioxide that inhibit the growth of microorganisms.^{23,24} The disadvantages of these materials are that they can be difficult and expensive to synthesize industrially, hazardous to the environment, and eventually lose their antimicrobial mechanism(s) over time. A potent, cost-efficient, scalable, environmentally friendly, and user-friendly material would fill an important need in minimizing the surface transmission of opportunistic fungi.

The results from Chapter 2 demonstrated that antimicrobial photodynamic therapy (aPDT) is a potential treatment for fungal infections. In that work and under a number of conditions examined, aPDT was able to completely eradicate fungi at low concentrations of cationic and anionic photosensitizers in solution. In a material-based approach, however, much less research in aPDT has been performed. Of note, Durantini and co-workers showed that the photodynamic inactivation of *C. albicans* using polysilsesquioxane films doped with 5-(4-carboxyphenyl)-10,15,20-tris(4-methylphenyl)porphyrin was able to achieve ~2.5 log

units CFU reduction after 1 hr of light illumination with a fluence of 320 J/cm².²⁵ Krausz and co-workers have also shown the photoinactivation of bacteria with porphyrin and chlorin photosensitizers incorporated into cellulose esterified plastic films.²⁶⁻²⁹ This latter work is of particularly relevance as we are interested in cellulose as a potential scaffold for antimicrobial materials. Cellulose is one of the most abundant and well-characterized biomaterials on Earth.³⁰ Cellulose consists of β -1,4-linked anhydro-D-glucose polymer chains, which afford it regions of repeating, regular crystalline units. Upon its acid hydrolysis, rod-shaped cellulose nanocrystals (CNCs) possessing unique properties are obtained. These CNCs also contains a primary hydroxymethyl group on their surface which allows for chemical modification and covalent attachment of pendant molecules.³⁰⁻³² The surface modifiable groups are advantageous in that they can potentially impart permanent antimicrobial properties to the resulting cellulose-photosensitizer conjugate, minimize biocide leaching, and prevent porphyrin aggregation.

Previously, our research group was able to covalently attach a tricationic alkyne-containing porphyrin onto the CNC surface via the Cu(I) catalyzed Huisgen-Meldal-Sharpless 1,3-dipolar cycloaddition reaction (a “Click reaction”), yielding CNC-CatPor.^{29,33} aPDT with CNC-CatPor demonstrated promising results on various Gram-positive and Gram-negative drug-resistant bacterial strains.^{34,35} However, the antifungal efficacy of this material was not investigated at that time. In this study, we explored the susceptibility of two pathogenic yeast strains of relevance to HAIs, *C. albicans* and *C. neoformans*, toward cellulose nanocrystals that contained covalently linked cationic (CNC-CatPor) and anionic (CNC-AnPor) porphyrins as photosensitizers. The photodynamic efficacies were determined

as a function of porphyrin loading onto the CNCs. The goal of this research was to investigate the potential for cellulose nanocrystals, when appropriately modified with photosensitizers, to be a suitable scaffold for antifungal materials. We were also motivated to find a better understanding of the PDT inactivation mechanism between different yeast genera. To the best of our knowledge, this is the first study using a cellulose nanomaterial for the photodynamic inactivation of pathogenic fungi.

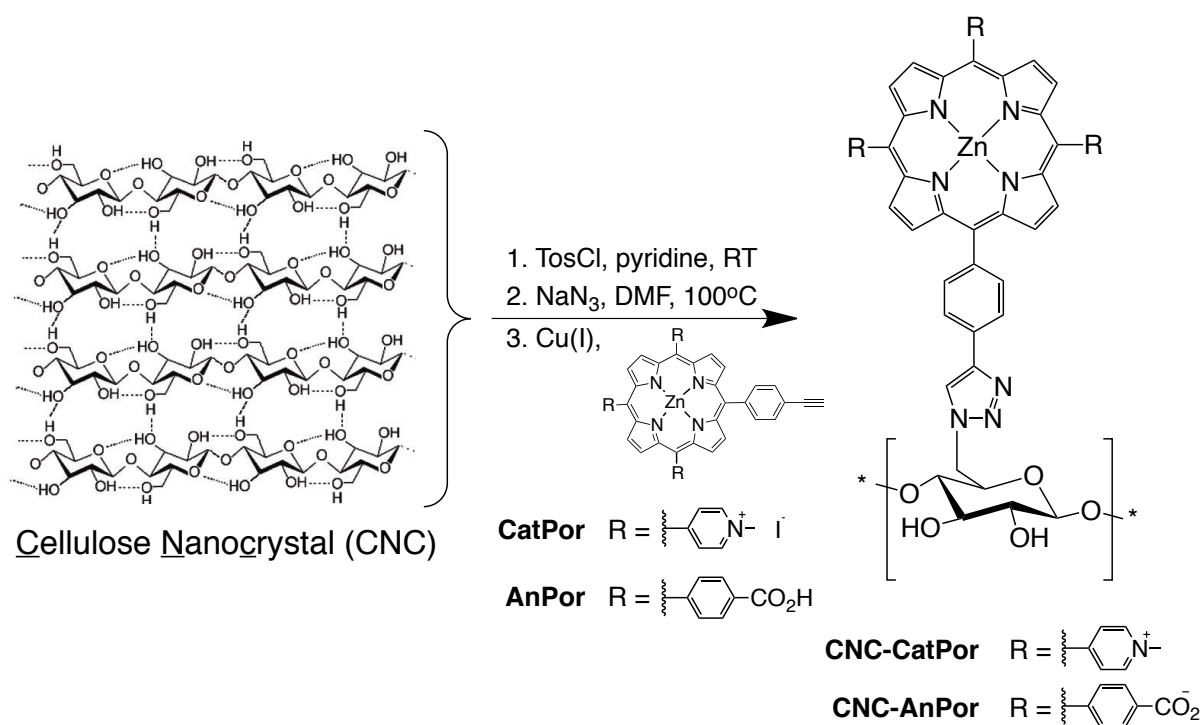


Figure 3.1. Synthesis of cellulose nanocrystal-porphyrin (CNC-por) conjugates.

3.3 Materials and Methods

CNC-porphyrin Preparation. CNC-CatPor and CNC-AnPor were prepared by Bradley Carpenter. The porphyrin loading onto the CNCs was determined by ICP-mass spectrometry (Environmental and Agricultural Testing Service, North Carolina State University). 10 mg of lyophilized CNC-por was digested in 10 mL of 1 M HCl and heated to 60 °C for 2 hrs. After 2 hrs, the porphyrin was assumed to be fully demetallated and the Zn²⁺ concentration was determined by ICP-MS. It was also assumed that the concentration of the Zn ion was equivalent to the porphyrin loading on CNC under complete porphyrin metallation. The porphyrin loadings for CNC-CatPor and CNC-AnPor were 0.14 and 0.05 μmoles porphyrin/mg of CNC-por respectively. Based on the porphyrin loading determined by ICP-MS, a 1 mM CNC-por stock solution of each material was prepared in ultrapure water, and were kept in the dark at 4 °C.

Strains and Culture Conditions. *Candida albicans* (ATCC 90028) and *Cryptococcus neoformans* (ATCC 64538) were obtained from the American Type Culture Collection (ATCC, Manassas, VA). Cell cultures were inoculated in growth media (yeast peptone dextrose (YPD) broth for *C. albicans* and Sabouraud dextrose (SD) broth for *C. neoformans*), followed by incubation at 37 °C overnight for *C. albicans*, or 48 hrs at 30 °C for *C. neoformans*. Cells were washed twice via sequential centrifugation (10 min, 3716 x g) and resuspension in phosphate buffer saline (PBS: 170 mM NaCl, 3.4 mM KCl, 10.0 mM Na₂HPO₄, 1.8 mM KH₂PO₄, pH 7.2) to remove excess media. The cells were then diluted in PBS to a cell concentration of ~2.0x10⁷ colony forming units (CFU) per mL as determined

by spectrophotometry at 600 nm (OD₆₀₀, Genesys 10 UV scanning spectrophotometer, Thermo Electron Corp).

Cell Incubation and Illumination Conditions with CNC-por. A 1 mL aliquot of the fungal cell culture was kept in the dark to serve as a compound-free dark control (-compound/-light). A suspension of CNC-por (10-200 μ M) was added to 4 mL of cell culture. The cell cultures were incubated in the dark at room temperature for 1 hr and agitated by a vortex mixer at the lowest speed. After 1 hr of incubation, three 1 mL aliquots of the cell suspension containing CNC-por were added to a sterile 24-well plate and illuminated for 30 min under constant stirring with visible light (400-700 nm) at 65 ± 5 mW/cm² (corresponding to a fluence of 108 J/cm²). The remaining cell suspension with CNC-por was shielded from light and kept as a +compound/-light dark control. All PDT experiments were performed using a non-coherent light source, PDT light model LC122 (LumaCare, U.S.A), and the fluence was determined by an Orion power meter (Orphir Optronics Ltd., Israel).

Cell Incubation and Illumination Conditions with Solution-Based Porphyrins. The cells were incubated in the dark with a 0.1, 1 or 10 μ M concentration of the photosensitizer, either CatPor or AnPor, for 30 mins. Then three 1 mL aliquots of the cell suspension were transferred to a sterile 24-well plate and illuminated with visible light (400-700 nm) for 15 or 30 mins under constant stirring at 65 ± 5 mW/cm² (corresponding to fluences of 54 and 108 J/cm²). Aliquots of cell cultures with and without compound were kept in the dark as controls.

Cell Survival Assays. After illumination, the -compound/-light control, +compound/-light control, and the +compound/+light treated cells were serially diluted 1:10 six times, and

plated on agar plates (YPD agar for *C. albicans* and SD agar for *C. neoformans*). The plates were incubated in the dark at 37 °C for 24 hours (*C. albicans*) or 30 °C for 48 hours (*C. neoformans*). All experiments were conducted in triplicate. Cell survival was determined based on the ratio of the CFU count between illuminated cells and the -compound/-light control. Under the conditions of our assay, the detection limit was set to 0.001%.

3.4 Results and Discussion

Photodynamic efficacies of CNC-CatPor and CNC-AnPor were investigated against *C. albicans* and *C. neoformans* in a concentration-dependent manner. The photoactivity of the water-soluble precursor compounds, CatPor and AnPor, were also studied. The porphyrin loading on the cellulose nanocrystals was determined by ICP-MS assaying for zinc ion. It was assumed that the zinc concentration thus determined was equivalent to the concentration of porphyrin loaded on the cellulose material. The final concentration refers to the concentration of porphyrin loaded on CNC in the insoluble suspension. In all experiments, yeast cells were incubated in the dark with CNC-por for 1 hr at room temperature under constant agitation by vortex mixer, followed by illumination (400-700 nm) at 65 ± 5 mW/cm² for 30 min (total fluence of 118 J/cm²). Cell survival rates were measured based on the viability of samples treated with light relative to the dark control in the absence of CNC-por. Different degrees of cell inactivation were observed for the two yeast strains studied for both CNC-CatPor and CNC-AnPor (Figs 3.2-3.7).

3.4.1 aPDT Studies with CatPor and CNC-CatPor

The photodynamic inactivation of *C. albicans* against CatPor and CNC-CatPor are shown in Figures 3.2A and 3.2B, respectively. Effective photoinactivation was observed for CatPor, with nearly detection limit inactivation (99.999%) when incubated with 1 μ M of the PS followed by 15 min light illumination. For CNC-CatPor, photoinactivation increased in a concentration-dependent manner. At 30 μ M CNC-CatPor suspension, a 2 log unit reduction in CFU was observed after 30 min illumination, and a 4 log unit CFU reduction was observed at 75 μ M. These results suggested that direct binding/uptake of the PS was not necessary for effective *C. albicans* inactivation given its covalent attachment to the CNCs. As the water-soluble cationic porphyrin showed detection limit inactivation at 1 μ M and 15 min illumination (~75-fold lower in concentration for the same level of photoinactivation when compared with CNC-CatPor), we conclude that this difference between CatPor and CNC-CatPor was likely due to the water-soluble PS binding to the cell surface or being uptaken into the cell, whereas the material-based CNC-CatPor produced reactive oxygen species that had to diffuse through the PBS buffer (<250 nm for $^1\text{O}_2$ to ~1.5 mm for H_2O_2) for sufficient cell inactivation.³⁶⁻³⁸

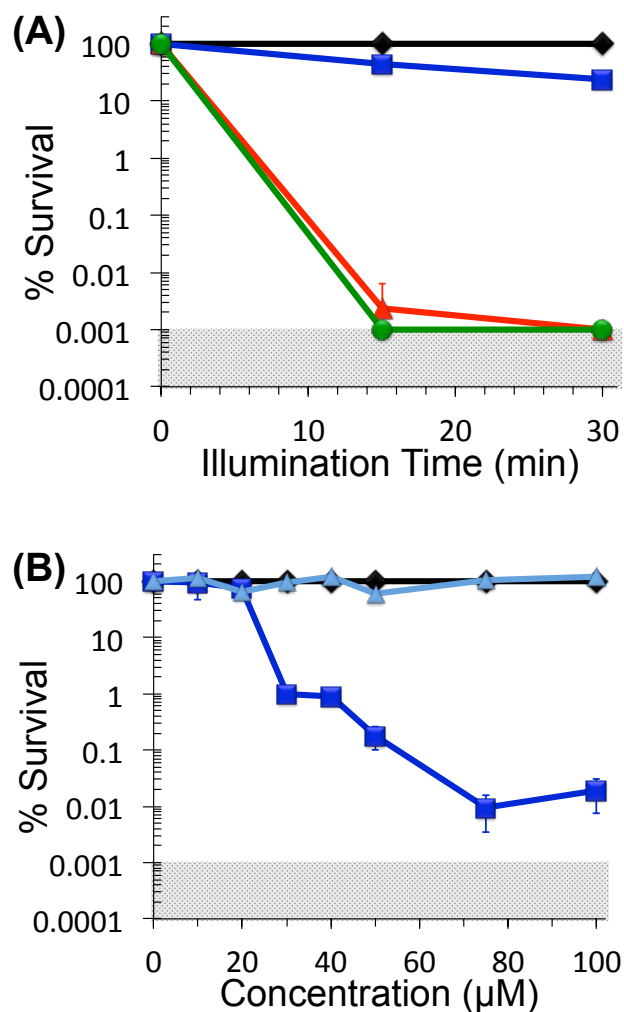


Figure 3.2. Photodynamic inactivation of *Candida albicans* with (A) water-soluble CatPor and (B) CNC-CatPor. (A) % survival for -compound/-light control (◆), 100 nM (■), 1 µM (▲), and 10 µM (●) CatPor. Cells were incubated with the photosensitizer for 30 min and illuminated (400-700 nm) at 65 ± 5 mW/cm² for 15 or 30 min (corresponding to total fluences of 59 and 118 J/cm²). (B) % survival for -compound/-light control (◆), +compound/-light control (▲), and light treated samples (■) with insoluble CNC-CatPor suspended in PBS to a final concentration between 10 to 100 µM. Cells treated with CNC-CatPor were incubated for 1 hr and illuminated with non-coherent light (400-700 nm) at 65 ± 5 mW/cm² for 30 min (fluence rate of 118 J/cm²). The detection limit was set to 0.001% survival.

The photodynamic efficacies of CatPor and CNC-CatPor against *C. neoformans* are shown in Fig. 3.3. The water-soluble CatPor exhibited 99.99% CFU reduction when tested against *C. neoformans* at 1 μM with 30 min of illumination, and reached detection-limit inactivation when the concentration was increased to 10 μM with 15 min illumination. By contrast, *C. neoformans* exhibited only a 0.5 log unit CFU reduction at 100 μM CNC-CatPor with 30 min of light treatment. Even after increasing the CNC-CatPor concentration to 200 μM , only a 1 log unit CFU reduction was observed. Thus, photoinactivation of *C. neoformans* was not effective with the immobilized PS, and suggested that direct binding of the PS was essential for effective *C. neoformans* inactivation. Regarding the differential level of photoinactivation between the two fungal strains, we attribute the observed results to the differences in membrane composition between the two: *C. neoformans* contains an outer cell membrane which *C. albicans* does not. This outer membrane is mainly comprised of polysaccharides which have been shown to be an integral part of the *C. neoformans* defense mechanism.³⁹⁻⁴² The capsule thickness for *C. neoformans* varies between 1 to 50 μm , depending on the cell type, environment, and growth conditions.⁴³ Yoneda and Doering showed that *C. neoformans* incubated for 48 hrs at 30 °C (the growth condition we employed in this study) had an average of 1.60 ± 0.19 μm of capsule thickness.⁴⁴ As singlet oxygen, the reactive oxygen species produced by PDT, is known to diffuse over 100-200 nm in water and 1 mm in air,³⁶ we suggest that the diffusion distance for $^1\text{O}_2$ is not sufficient enough to travel through the polysaccharide capsule of *C. neoformans* for efficient cell inactivation when generated from the immobilized PS.

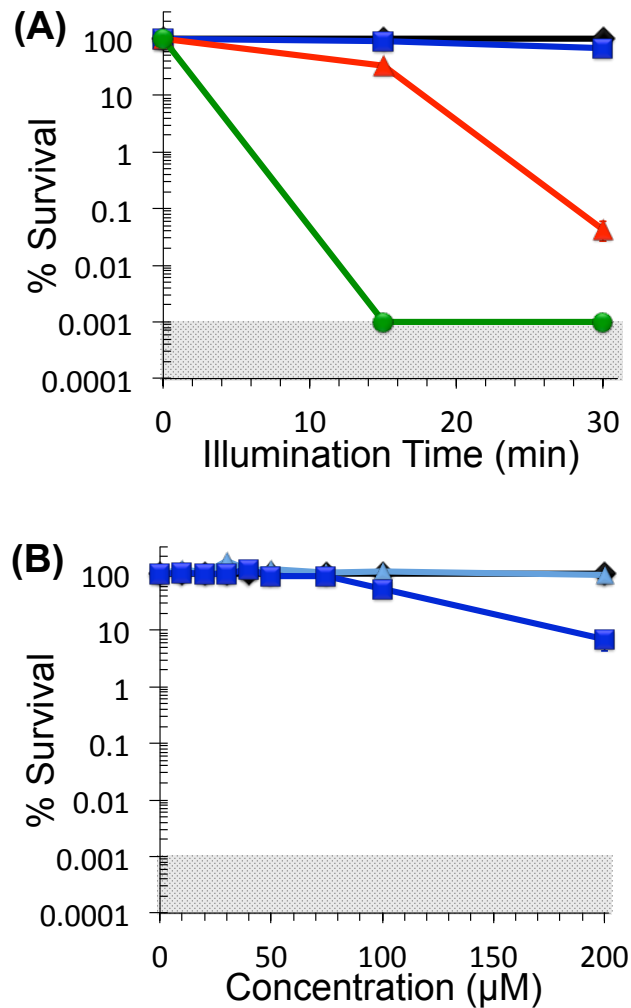


Figure 3.3. Photodynamic inactivation of *C. neoformans* with (A) water-soluble CatPor and (B) CNC-CatPor. (A) % survival for -compound/-light control (◆), 100 nM (■), 1 µM (▲), and 10 µM (●) CatPor. Cells were incubated with photosensitizer for 30 min and illuminated (400-700 nm) at 65 ± 5 mW/cm² for 15 or 30 min (corresponding to total fluences of 59 and 118 J/cm²). (B) % survival for -compound/-light control (◆), for +compound/-light control (▲) and light treated samples (■) with insoluble CNC-CatPor suspended in PBS to a final concentration between 10-200 µM. Cells treated with CNC-CatPor were incubated for 1 hr and illuminated with non-coherent light (400-700 nm) at 65 ± 5 mW/cm² for 30 min (fluence rate of 118 J/cm²). The detection limit was set to 0.001% survival.

Photoinactivation of *C. neoformans* with 200 μM of CNC-CatPor (Fig. 3.4) with a longer illumination time of 1 hr led to detection-limit eradication of the cells. A possible explanation for this 4 log unit improvement in cell inactivation when compared to the 30 min time point could be that the longer illumination time allowed for reactive oxygen species produced during the early part of the illumination period to degrade the outer polysaccharide capsule of *C. neoformans*, allowing for singlet oxygen produced in the later part of the illumination period to more directly interact with the cells.

To further explore the mode of action of the CNC-CatPor material, we examined if solubilized fragments of CNC-CatPor played a role in the aPDT of *C. neoformans*. A 200 μM suspension of CNC-CatPor was centrifuged, the supernatant separated, and the resulting material was resuspended in PBS. Both the resuspended CNC-CatPor and the supernatant were each incubated with *C. neoformans* for 1 hr followed by illumination (400-700 nm, 65 mW/cm^2 , 1 hr). The photodynamic inactivation for each demonstrated a ~ 2.5 log unit CFU reduction (Figure 3.4). The fact that the supernatant derived from the 200 μM CNC-CatPor suspension was able to photoinactivate *C. neoformans* suggested that PS leaching might occur at high PS concentration. This could be due to insufficient washing of the material to remove unreacted PS during the synthesis of CNC-CatPor, or more likely due to the presence of low MW CNC fragments that contain covalently attached PS. CNC-CatPor without the supernatant was still able to photoinactivate *C. neoformans* (2.5 log unit CFU reduction), demonstrating the potency of this material.

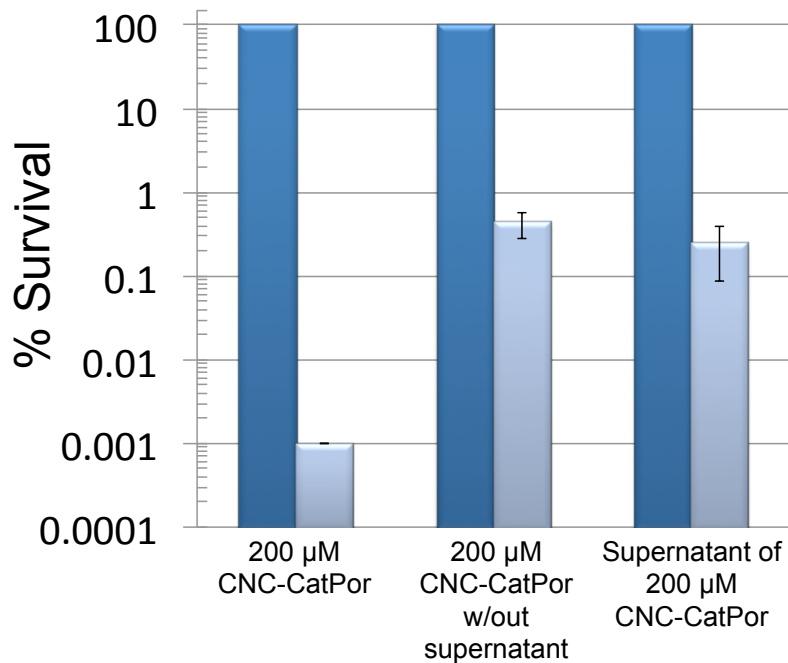


Figure 3.4. Photodynamic inactivation of *C. neoformans* with 200 μ M of CNC-CatPor. Dark control (■) and samples treated with light (▒). Cells were incubated with 200 μ M CNC-CatPor with and without its resuspended supernatant, and with the supernatant itself, for 1 hr followed by 1 hr of illumination with visible light (400-700 nm) at 65 ± 5 mW/cm².

3.4.2 aPDT Studies with AnPor and CNC-AnPor

C. albicans was inactivated to the detection limit (99.999%) upon PDT treatment with 30 μ M CNC-AnPor suspension and 30 min illumination (Fig. 3.5). CNC-AnPor showed no toxicity to *C. albicans* in the dark (Fig 3.5B). Even as low as 10 or 20 μ M of CNC-AnPor suspensions, 2 and 3 log units reduction in viable cells were achieved, respectively. By contrast, as low as 1 μ M of the solution-based AnPor with 30 min of illumination was needed to reach detection limit inactivation for *C. albicans* (a 30-fold lower concentration when

compared to its CNC conjugate). Overall, the photoinactivation studies demonstrated that *C. albicans* is highly susceptible to both AnPor and CNC-AnPor.

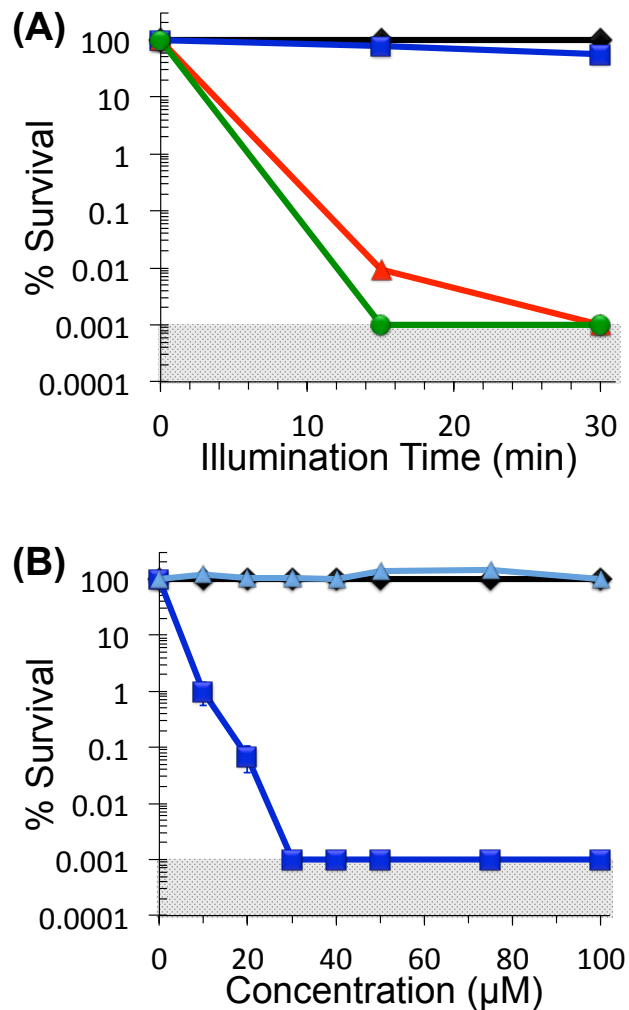


Figure 3.5. Photodynamic inactivation of *C. albicans* with (A) water soluble AnPor and (B) CNC-AnPor. (A) % survival for -compound/-light control (◆) and light-treated samples with 100 nM (■), 1 µM (▲), and 10 µM (●) of AnPor after illumination (400-700 nm) at 65 ± 5 mW/cm² for 15 or 30 min (corresponding to total fluences of 59 and 118 J/cm²). (B) % survival for -compound/-light control (◆), +compound/-light control (▲), and light treated samples (■) with insoluble CNC-AnPor suspended in PBS to a final concentration between 10-100 µM. Cells treated with CNC-AnPor were incubated for 1 hr and illuminated with non-coherent light (400-700 nm) at 65 ± 5 mW/cm² for 30 min (fluence rate of 118 J/cm²). The detection limit was set to 0.001% survival.

As investigated above for CNC-CatPor, we examined if solubilized fragments of CNC-AnPor played a role in the aPDT of *C. albicans*. A 30 μM suspension of CNC-AnPor was centrifuged, the supernatant separated, and the resulting material was resuspended in PBS. Both the resuspended CNC-AnPor and the supernatant were each incubated with *C. albicans* for 1 hr followed by 30 min of illumination under our standard conditions. The photodynamic inactivation by the resuspended CNC-AnPor exhibited a ~ 4.5 log unit CFU reduction, whereas the supernatant only yielded a ~ 1 log unit reduction in CFU (Figure 3.6). These results suggested that CNC-AnPor, and not solubilized fragments, was responsible for the majority of the photoinactivation observed here.

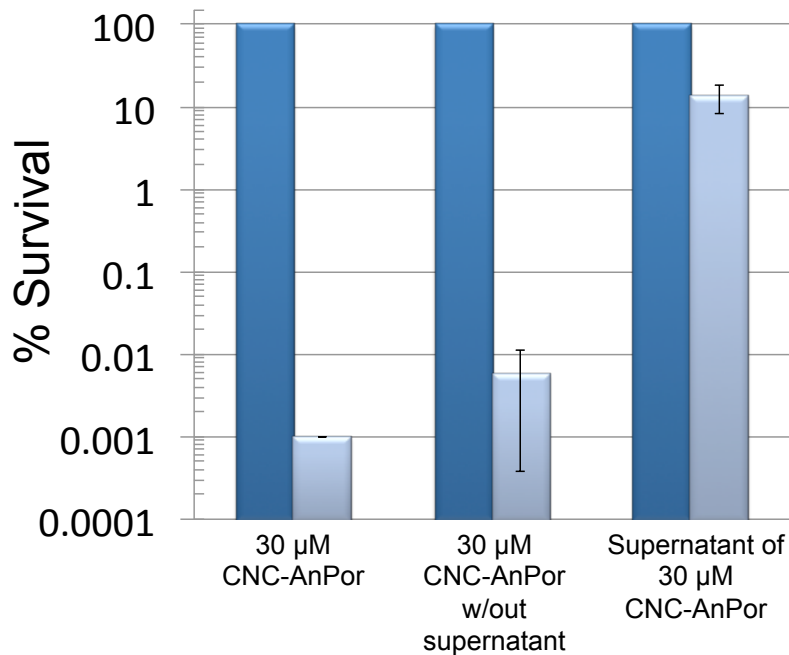


Figure 3.6. Photodynamic inactivation of *C. albicans* with 30 μM CNC-AnPor. Dark control (■) and samples treated with light (□). Cells were incubated with 30 μM CNC-AnPor with and without its resuspended supernatant, and with the supernatant itself, for 1 hr followed by 1 hr of illumination with visible light (400-700 nm) at 65 ± 5 mW/cm^2 .

Susceptibility of *C. neoformans* towards AnPor was minimal (Fig. 3.7A). Even at a relatively high concentration of 10 μ M, only a 2 log unit CFU reduction was observed for *C. neoformans*. The outer membrane of *C. neoformans* is comprised of ~90% glucuronoxylomannan (GXM)⁴⁵ polysaccharides that are negatively charged, and it is likely for this reason (electrostatic repulsion) as to why *C. neoformans* was not susceptible towards AnPor. Interestingly, *C. neoformans* cultures incubated with a 20 μ M suspension of CNC-AnPor showed over a 4 log unit reduction (99.99%) in viable cells. While this initially suggested that CNC-AnPor may have an improved PDT ability compared to AnPor, the dark control culture of *C. neoformans* incubated with CNC-AnPor in the absence of any light exposure also showed CFU reduction of ~ 4 log units (Figure 3.7B). This suggested that cellulose nanocrystals are toxic to *C. neoformans* when covalently linked to an anionic porphyrin even without PDT treatment. Additional studies are needed to understand the non-PDT mode of action of CNC-AnPor for *C. neoformans* cell inactivation.

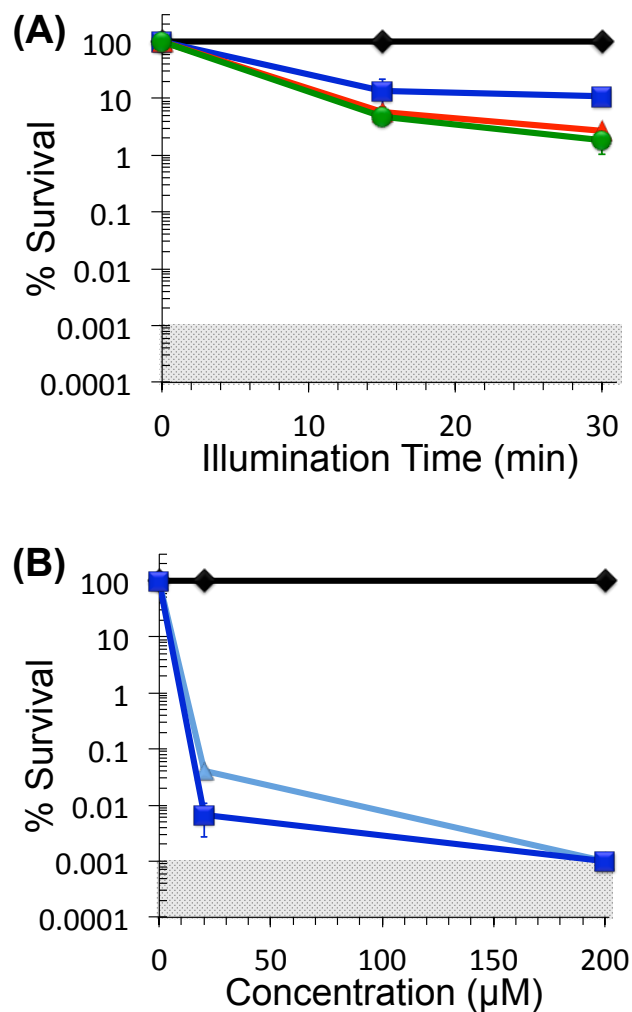


Figure 3.7. Photodynamic inactivation of *C. neoformans* with (A) water soluble AnPor and (B) CNC-AnPor. (A) % survival for -compound/-light control (◆) and light-treated samples with 100 nM (■), 1 µM (▲), and 10 µM (●) of AnPor after illumination (400-700 nm) at 65 ± 5 mW/cm² for 15 or 30 min (corresponding to total fluences of 59 and 118 J/cm²). (B) % survival for -compound/-light control (◆), +compound/-light control (▲), and light treated samples (■) with insoluble CNC-AnPor suspended in PBS to a final concentration between 10-200 µM. Cells treated with CNC-AnPor were incubated for 1 hr and illuminated with non-coherent light (400-700 nm) at 65 ± 5 mW/cm² for 30 min (fluence rate of 118 J/cm²). The detection limit was set to 0.001% survival.

3.5 Conclusions

The photodynamic susceptibilities of two pathogenic fungal strains associated with HAIs, *C. albicans* and *C. neoformans*, using porphyrin-conjugated cellulose nanocrystals as photosensitizers were investigated in this study. The photodynamic efficacy of the solution-based AnPor and its CNC conjugate, CNC-AnPor, against *C. albicans* demonstrated that, in contrast to bacteria, anionic PS are able to effectively photoinactivate *C. albicans*. The PDI efficacy between solution-based PS and their CNC-conjugates was also investigated for *C. albicans*. The photoinactivation of *C. albicans* by CatPor is about 100-fold greater than its CNC conjugate, and photoinactivation by AnPor is ~30-fold greater than its CNC conjugate. Such differences between solution based PS and their immobilized conjugates should be taken into consideration for CNC surface tuning and modification.

Photoinactivation of *C. neoformans* by CNC-CatPor was highly dependent upon illumination time, a result that could relate to the capsule thickness on the cell membrane. Studies of the photoinactivation of *C. neoformans* as a function of different growth conditions may provide a firmer understanding of the role of capsule thickness in PDT inactivation. Surprisingly, *C. neoformans* was able to be fully inactivated to the detection limit with 20 μM CNC-AnPor in the absence of light, suggesting that this material is itself an antifungal agent. Overall, these results provide the foundation for understanding the mechanism of *C. albicans* and *C. neoformans* (photo)inactivation, and provide guidance for the future chemical modification of CNCs.

REFERENCES

- (1) Klevens, R. M.; Edwards, J. R.; Richards, C. L., Jr.; Horan, T. C.; Gaynes, R. P.; Pollock, D. A.; Cardo, D. M. *Public Health Rep* **2007**, *122*, 160.
- (2) Moan, J. *Photochem Photobiol* **1986**, *43*, 681.
- (3) Feese, E.; Ghiladi, R. A. *J Antimicrob Chemoth* **2009**, *64*, 782.
- (4) Pittet, D.; Tarara, D.; Wenzel, R. P. *JAMA* **1994**, *271*, 1598.
- (5) Edmond, M. B.; Wallace, S. E.; McClish, D. K.; Pfaller, M. A.; Jones, R. N.; Wenzel, R. P. *Clin Infect Dis* **1999**, *29*, 239.
- (6) Gudlaugsson, O.; Gillespie, S.; Lee, K.; Vande Berg, J.; Hu, J.; Messer, S.; Herwaldt, L.; Pfaller, M.; Diekema, D. *Clin Infect Dis* **2003**, *37*, 1172
- (7) Wenzel, R. P. *Clin Infect Dis* **1995**, *20*, 1531.
- (8) Gonzalez de Molina, F.; Leon, C.; Ruiz-Santana, S.; Saavedra, P.; Group, t. C. I. S. *Critical Care* **2012**, *16*, R105.
- (9) Nolla-Salas, J.; Sitges-Serra, A.; Leon-Gil, C.; Martinez-Gonzalez, J.; Leon-Regidor, M.; Ibanez-Lucia, P.; Torres-Rodriguez, J. *Intensive Care Med* **1997**, *23*, 23
- (10) Currie, B. P.; Casadevall, A. *Clin Infect Dis* **1994**, *19*, 1029.
- (11) Mitchell, T. G.; Perfect, J. R. *Clin Microbiol Rev* **1995**, *8*, 515.
- (12) Ammerlaan, H. S.; Harbarth, S.; Buiting, A. G.; Crook, D. W.; Fitzpatrick, F.; Hanberger, H.; Herwaldt, L. A.; van Keulen, P. H.; Kluytmans, J. A.; Kola, A.; Kuchenbecker, R. S.; Lingaas, E.; Meessen, N.; Morris-Downes, M. M.; Pottinger, J. M.; Rohner, P.; dos Santos, R. P.; Seifert, H.; Wisplinghoff, H.; Ziesing, S.; Walker, A. S.; Bonten, M. J. *Clin Infect Dis* **2013**, *56*, 798.
- (13) Sauvet, G.; Fortuniak, W.; Kazmierski, K.; Chojnowski, J. *J Polym Sci Pol Chem* **2003**, *41*, 2939.
- (14) Vigo, T. L. *Advances in Antimicrobial Polymers and Materials*; Plenum Press, 1994.
- (15) Kenawy, E. R.; Abdel-Hay, F. I.; El-Shanshoury, A. E. R. R.; El-Newehy, M. H. *J Polym Sci Pol Chem* **2002**, *40*, 2384.

- (16) Cen, L.; Neoh, K. G.; Kang, E. T. *Langmuir* **2003**, *19*, 10295.
- (17) Viscardi, G.; Quagliotto, P.; Barolo, C.; Savarino, P.; Barni, E.; Fiscaro, E. *J Org Chem* **2000**, *65*, 8197.
- (18) Krishnan, S.; Ward, R. J.; Hexemer, A.; Sohn, K. E.; Lee, K. L.; Angert, E. R.; Fischer, D. A.; Kramer, E. J.; Ober, C. K. *Langmuir* **2006**, *22*, 11255.
- (19) Zumbuehl, A.; Ferreira, L.; Kuhn, D.; Astashkina, A.; Long, L.; Yeo, Y.; Iaconis, T.; Ghannoum, M.; Fink, G. R.; Langer, R.; Kohane, D. S. *Proc Natl Acad Sci U S A* **2007**, *104*, 12994.
- (20) Kaczmarek, H.; Bajer, K. *J Polym Sci, Part B: Polym Phys* **2007**, *45*, 903.
- (21) Dawson-Andoh, B.; Matuana, L. M.; Harrison, J. *J Vinyl Addit Techn* **2004**, *10*, 179.
- (22) Kositchaiyong, A.; Rosarpitak, V.; Sombatsompop, N. *Polym Eng Sci* **2013**, n/a.
- (23) Chung, C.-J.; Lin, H.-I.; Tsou, H.-K.; Shi, Z.-Y.; He, J.-L. *J Biomed Mater Res, Part B* **2008**, *85B*, 220.
- (24) Souli, M.; Galani, I.; Plachouras, D.; Panagea, T.; Armaganidis, A.; Petrikkos, G.; Giamarellou, H. *J Antimicrob Chemother* **2013**, *68*, 852.
- (25) Alvarez, M. G.; Gomez, M. L.; Mora, S. J.; Milanesio, M. E.; Durantini, E. N. *Bioorg Med Chem* **2012**, *20*, 4032.
- (26) Krouit, M.; Granet, R.; Branland, P.; Verneuil, B.; Krausz, P. *Bioorg Med Chem Lett* **2006**, *16*, 1651.
- (27) Krouit, M.; Granet, R.; Krausz, P. *Bioorg Med Chem* **2008**, *16*, 10091.
- (28) Krouit, M.; Granet, R.; Krausz, P. *Eur Polym J* **2009**, *45*, 1250.
- (29) Tornøe, C. W.; Christensen, C.; Meldal, M. *J Org Chem* **2002**, *67*, 3057.
- (30) Habibi, Y.; Lucia, L. A.; Rojas, O. J. *Chem Rev* **2010**, *110*, 3479.
- (31) Ranby, B. G. *Discuss Faraday Soc* **1951**, 158.
- (32) Filpponen, I.; Argyropoulos, D. S. *Biomacromolecules* **2010**, *11*, 1060.

- (33) Rostovtsev, V. V.; Green, L. G.; Fokin, V. V.; Sharpless, K. B. *Angew Chem Int Ed Engl* **2002**, *41*, 2596.
- (34) Feese, E.; Sadeghifar, H.; Gracz, H. S.; Argyropoulos, D. S.; Ghiladi, R. A. *Biomacromolecules* **2011**, *12*, 3528.
- (35) Carpenter, B. L.; Feese, E.; Sadeghifar, H.; Argyropoulos, D. S.; Ghiladi, R. A. *Photochem Photobiol* **2012**, *88*, 527.
- (36) Midden, W. R.; Wang, S. Y. *J Am Chem Soc* **1983**, *105*, 4129.
- (37) Redmond, R. W.; Gamlin, J. N. *Photochem Photobiol* **1999**, *70*, 391.
- (38) Winterbourn, C. C. *Nat Chem Biol* **2008**, *4*, 278.
- (39) Bulmer, G. S.; Sans, M. D.; Gunn, C. M. *J Bacteriol* **1967**, *94*, 1475.
- (40) Kozel, T. R.; Pfrommer, G. S.; Guerlain, A. S.; Highison, B. A.; Highison, G. J. *Rev Infect Dis* **1988**, *10 Suppl 2*, S436.
- (41) Zaragoza, O.; Telzak, A.; Bryan, R. A.; Dadachova, E.; Casadevall, A. *Mol Microbiol* **2006**, *59*, 67.
- (42) Hamilton, A. J.; Goodley, J. *Curr Top Med Mycol* **1996**, *7*, 19.
- (43) McFadden, D. C.; De Jesus, M.; Casadevall, A. *J Biol Chem* **2006**, *281*, 1868.
- (44) Yoneda, A.; Doering, T. L. *Eukaryot Cell* **2008**, *7*, 546.
- (45) Vartivarian, S. E.; Reyes, G. H.; Jacobson, E. S.; James, P. G.; Cherniak, R.; Mumaw, V. R.; Tingler, M. J. *J Bacteriol* **1989**, *171*, 6850.